



Detection of DEfects and HYDROgen by ion beam analysis in Channeling mode for fusion – DeHydroC

Project code: ENR-MAT-01-JSI

Reporting meeting - activities 2023
6. February 2024

Sabina Markelj (PI) on behalf of the team



Team members



MAX-PLANCK-INSTITUT
FÜR PLASMAPHYSIK

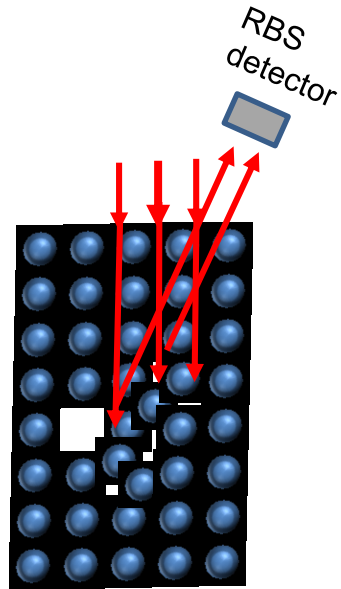


| Beneficiary | Names | Expertise | Contact |
|----------------|------------------------|---|--|
| JSI | Sabina Markelj | HI interaction, sample irradiation, ion beam analysis (IBA) | sabina.markelj@ijs.si |
| | Esther Punzón Quijorna | Channelling, IBA (Post-doc) | esther.punzon-quijorna@ijs.si |
| | Mitja Kelemen | Construction, IBA, channelling (PhD, Post-doc) | mitja.kelemen@ijs.si |
| | Matjaž Vencelj | Detectors | matjaz.vencelj@ijs.si |
| | Primož Pelicon | IBA, construction, channelling | Primož.Pelicon@ijs.si |
| | Janez Zavašnik | TEM/SEM | janez.zavasnik@ijs.si |
| | Andreja Šestan | TEM/SEM, sample preparation (PhD, Post-doc) | andreja.sestan@ijs.si |
| | MPG | Thomas Schwarz-Selinger | Sample irradiation, IBA, HI interaction, TDS |
| Wolfgang Jacob | | HI interaction, TDS | Wolfgang.Jacob@ipp.mpg.de |
| UHEL | Flyura Djurabekova | Multiscale modelling, RBSADEC development | flyura.djurabekova@helsinki.fi |
| | Xin Jin | Code development, MD, RBSADEC (PhD) | xin.jin@helsinki.fi |
| | Ilja Makkonen | DFT for RBSADEC (Post-doc) | Ilja.makkonen@helsinki.fi |
| | Tommy Ahlgren | IBA, HI interaction, MRE modelling | tommy.ahlgren@helsinki.fi |
| | Kenichiro Mizohata | IBA, RBS-channelling | kenichiro.mizohata@helsinki.fi |
| | Filip Tuomisto | PAS | filip.tuomisto@helsinki.fi |
| CEA | Christian Grisolia | MRE modelling | Christian.GRISOLIA@cea.fr |
| | Etienne Hodille | MRE modelling, MD | Etienne.HODILLE@cea.fr |



Methodology

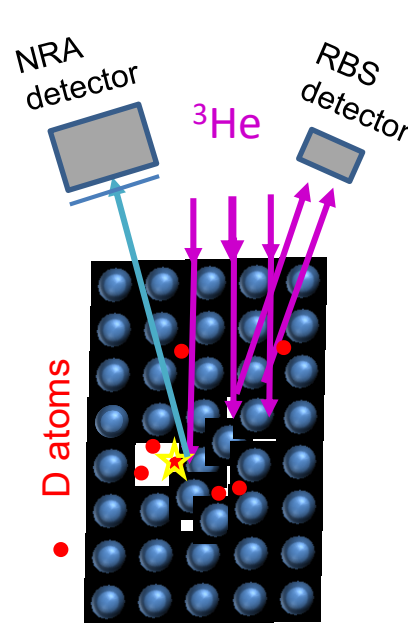
Channeling Rutherford Backscattering Spectroscopy (RBS - C)



- Ion beam techniques
- Non-destructive!
- In situ!

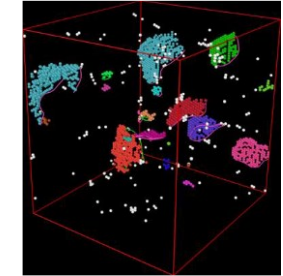
- Disorder in materials due to irradiation (depth resolved)
Defect type?
- Sensitive mainly to dislocation structure (loops, lines)

Nuclear Reaction Analysis (NRA - C)



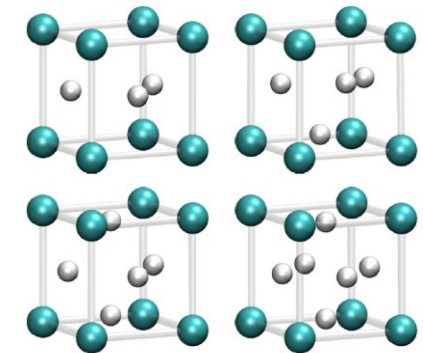
- Deuterium populates defects in materials – analysis depth resolved
Defect type?
- D traps mainly in open volume defects (vacancies, vacancy clusters)

Molecular Dynamics (MD)



- Collision cascades (~10–100 nm)
- High radiation dose

Density Functional Theory (DFT)



Heinola et al. PR B (2010)

- Hydrogen atom positions around vacancy/vacancy cluster

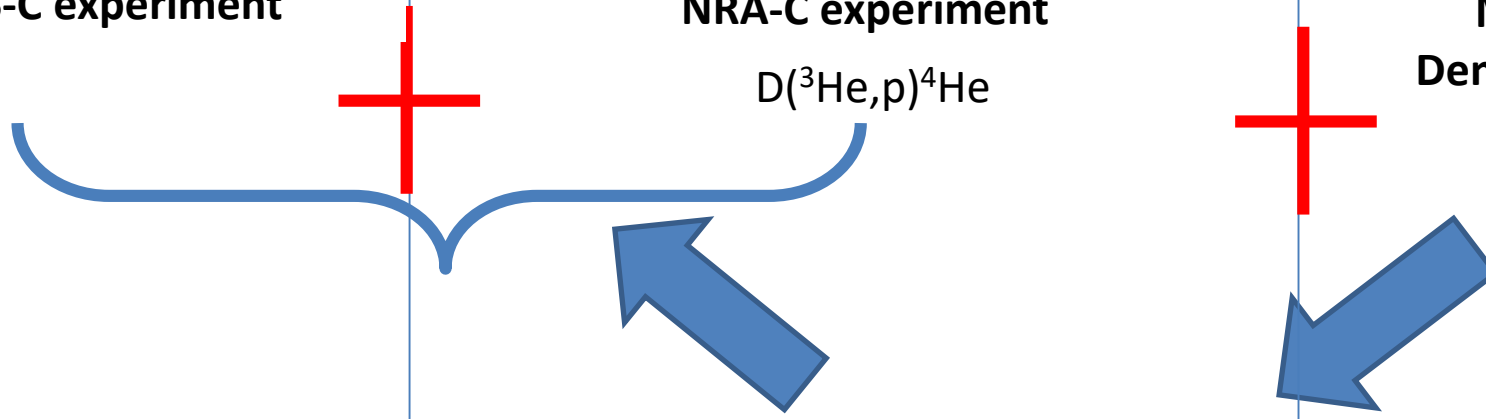


RBS-C experiment

NRA-C experiment

$D(^3\text{He},p)^4\text{He}$

Molecular Dynamics (MD)
Density Functional Theory (DFT)



RBS-C / NRA-C simulations
RBSADEC code

[S. Zhang *et al.*, *Phys. Rev. E*, 94 (2016) 043319]

Combination of MD, DFT
RBS-C, NRA-C experiments and
simulations



Defect types and deuterium locations!

Tasks and objectives in 2023



- Task 1.1 Incorporation of the goniometer in the INSIBA experimental station – JSI.
- Task 1.2 Detection system for ion beam methods
 - ❖ **O3.1 (Task 1.1) C-RBS spectra obtained with new channeling set-up. (D1)**
- Task 2.1 Production of samples with dominant defects in the material – MPG and JSI.
- Task 2.2 Characterization of defects –UHEL, JSI, MPG.
- Task 2.3 Simulation and interpretation of C-RBS spectra - UHEL, CEA, JSI.
 - ❖ **O3.2 (Task 2.2, 2.3, 3.1) Defect identification by C-RBS and correlation to TEM and PAS measurements – report. (D2)**
- Task 2.4 In-situ C-RBS and sample heating – JSI
 - ❖ **O3.3 (Task 2.4) In-situ sample heating in INSIBA-C. (M6)**
- Task 3.1 Characterization of defects by D retention studies and MRE modelling - JSI, MPG, CEA, UHEL.
- Task 3.2 Development of C-NRA method - JSI, UHEL, MPG.
 - ❖ **O3.4 (Task 3.1 and Task 3.2) Detection of deuterium by C-NRA method. (M8)**
- Task 3.3 – Modelling of deuterium position in lattice/defect and identification of D position - UHEL, CEA, JSI.
 - ❖ **O3.5 (Task 3.3) Incorporation of C-NRA in RBSADEC. (M9)**

Tasks and objectives in 2023



- Task 1.1 Incorporation of the goniometer in the INSIBA experimental station – JSI.
- Task 1.2 Detection system for ion beam methods
 - ❖ **O3.1 (Task 1.1)) C-RBS spectra obtained with new channeling set-up. (D1)**
- Task 2.1 Production of samples with dominant defects in the material – MPG and JSI.
- Task 2.2 Characterization of defects –UHEL, JSI, MPG.
- Task 2.3 Simulation and interpretation of C-RBS spectra - UHEL, CEA, JSI.
 - ❖ **O3.2 (Task 2.2, 2.3, 3.1) Defect identification by C-RBS and correlation to TEM and PAS measurements – report. (D2)**
- Task 2.4 In-situ C-RBS and sample heating – JSI
 - ❖ **O3.3 (Task 2.4) In-situ sample heating in INSIBA-C. (M6)**
- Task 3.1 Characterization of defects by D retention studies and MRE modelling - JSI, MPG, CEA, UHEL.
- Task 3.2 Development of C-NRA method - JSI, UHEL, MPG.
 - ❖ **O3.4 (Task 3.1 and Task 3.2) Detection of deuterium by C-NRA method. (M8)**
- Task 3.3 – Modelling of deuterium position in lattice/defect and identification of D position - UHEL, CEA, JSI.
 - ❖ **O3.5 (Task 3.3) Incorporation of C-NRA in RBSADEC. (M9)**



On schedule



Delayed



WP 4 management - four zoom meetings organized with the team members, details and presentations available on Indico, links to indico sites on Wiki page https://wiki.euro-fusion.org/wiki/Project_No4

- March 2023 – three-day meeting in Ljubljana, Slovenia
- June 2023
- September 2023
- December 2023

Publications:

- Jin et al., Effect of lattice voids on Rutherford backscattering dechanneling in tungsten, J. Phys. D: Appl. Phys. 56 (2023) 065303 (13pp) <https://doi.org/10.1088/1361-6463/acad12> ID: 33582
- Markelj et al., Unveiling the radiation-induced defect production and damage evolution in tungsten using multi-energy Rutherford backscattering spectroscopy in channeling configuration, Acta Materialia 263 (2024) 119499, <https://doi.org/10.1016/j.actamat.2023.119499> ID: 35374

Under review:

- Jin et al. Analysis of lattice location of deuterium in tungsten and its application for predicting deuterium trapping conditions, Submitted to PRM (Rejected at Acta Materialia) ID: 36157
- Markelj et al., First study of the location of deuterium in displacement damaged tungsten by nuclear reaction analysis in channeling configuration, Submitted to NME as ICFRM proceedings ID: 33906

In preparation:

- Zavašnik et al. Microstructural analysis of tungsten single crystals samples irradiated by W ions: the effect of dose and temperature on damage evolution

Tasks and objectives in 2023

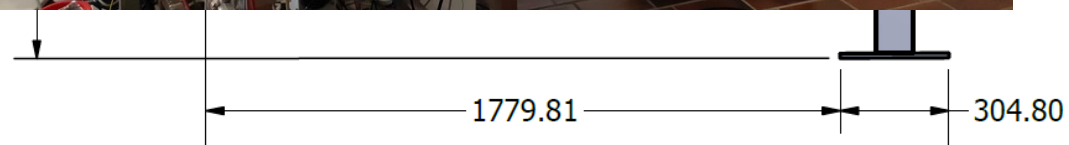
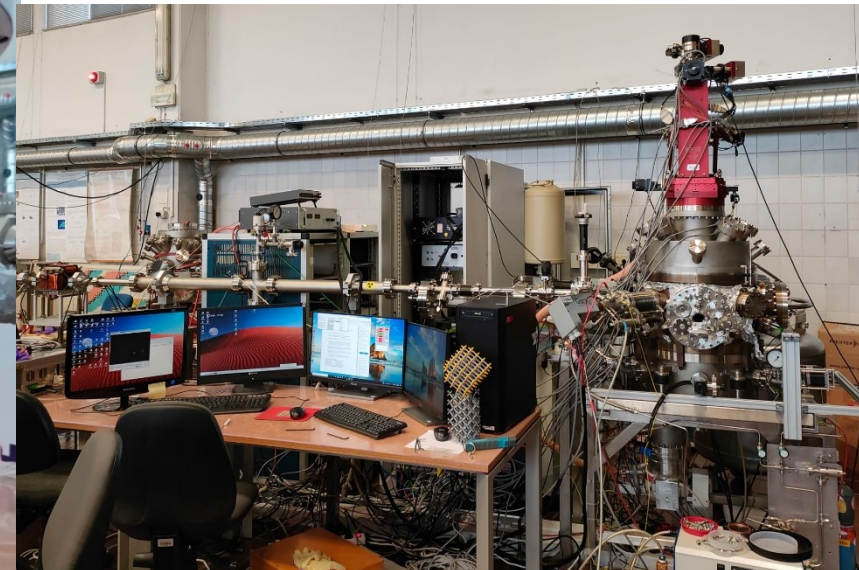
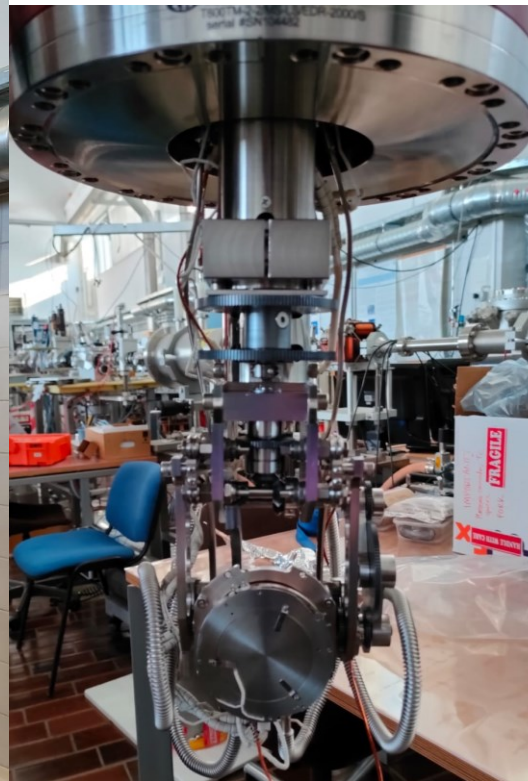
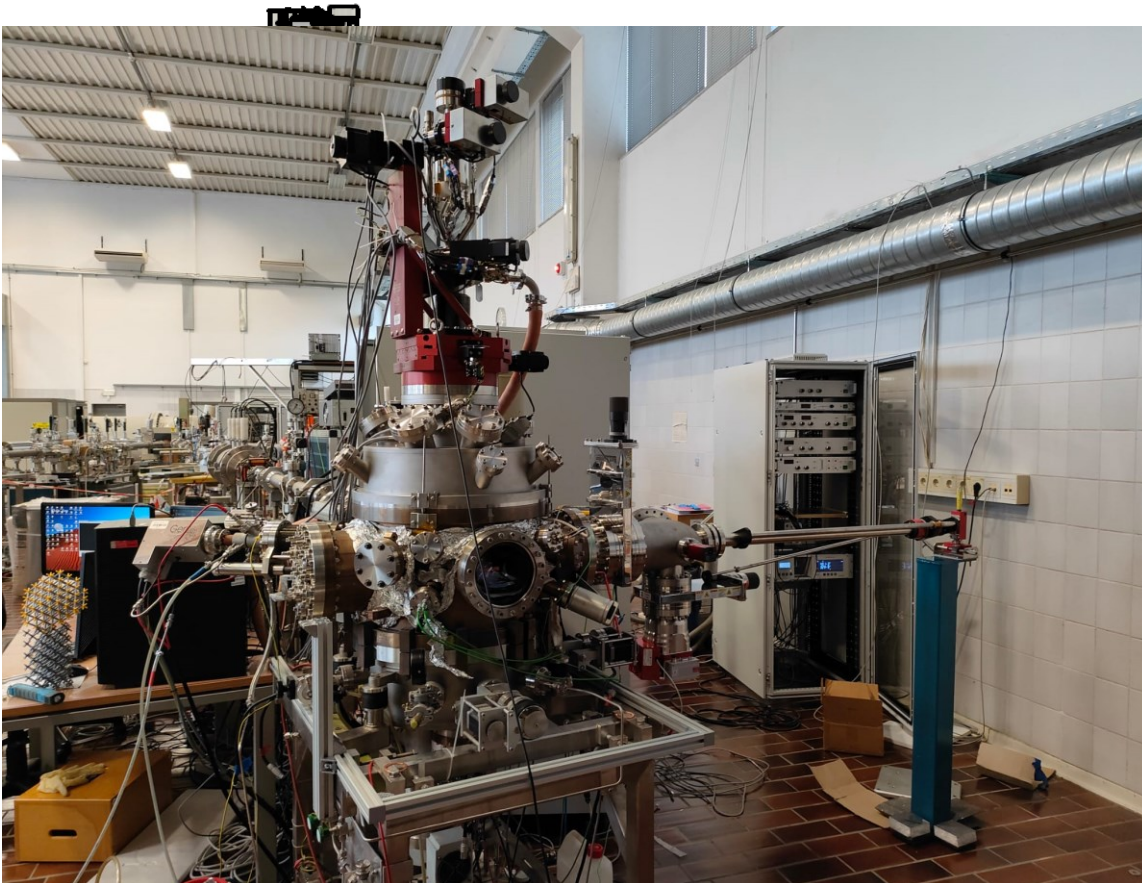


- Task 1.1 Incorporation of the goniometer in the INSIBA experimental station – JSI.
- Task 1.2 Detection system for ion beam methods
 - ❖ **O3.1 (Task 1.1) C-RBS spectra obtained with new channeling set-up. (D1)**
- Task 2.1 Production of samples with dominant defects in the material – MPG and JSI.
- Task 2.2 Characterization of defects –UHEL, JSI, MPG.
- Task 2.3 Simulation and interpretation of C-RBS spectra - UHEL, CEA, JSI.
 - ❖ **O3.2 (Task 2.2, 2.3, 3.1) Defect identification by C-RBS and correlation to TEM and PAS measurements – report. (D2)**
- Task 2.4 In-situ C-RBS and sample heating – JSI
 - ❖ **O3.3 (Task 2.4) In-situ sample heating in INSIBA-C. (M6)**
- Task 3.1 Characterization of defects by D retention studies and MRE modelling - JSI, MPG, CEA, UHEL.
- Task 3.2 Development of C-NRA method - JSI, UHEL, MPG.
 - ❖ **O3.4 (Task 3.1 and Task 3.2) Detection of deuterium by C-NRA method. (M8)**
- Task 3.3 – Modelling of deuterium position in lattice/defect and identification of D position - UHEL, CEA, JSI.
 - ❖ **O3.5 (Task 3.3) Incorporation of C-NRA in RBSADEC. (M9)**

6-axis goniometer



- ✓ JSI – 6-axis goniometer specified, public call, final order at National Electrostatic Corp. (NEC) 08/2021. Delivery scheduled for June 2022, delivery of last missing parts on 22nd January 2024!



Tasks and objectives in 2023

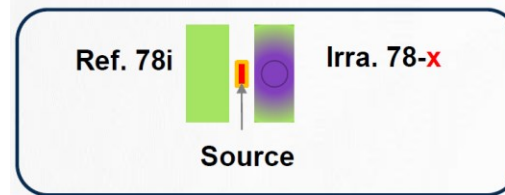


- Task 1.1 Incorporation of the goniometer in the INSIBA experimental station – JSI.
- Task 1.2 Detection system for ion beam methods
 - ❖ **O3.1 (Task 1.1) C-RBS spectra obtained with new channeling set-up. (D1)**
- Task 2.1 Production of samples with dominant defects in the material – MPG and JSI.
- **Task 2.2 Characterization of defects –UHEL, JSI, MPG.**
- Task 2.3 Simulation and interpretation of C-RBS spectra - UHEL, CEA, JSI.
 - ❖ **O3.2 (Task 2.2, 2.3, 3.1) Defect identification by C-RBS and correlation to TEM and PAS measurements – report. (D2)**
- Task 2.4 In-situ C-RBS and sample heating – JSI
 - ❖ **O3.3 (Task 2.4) In-situ sample heating in INSIBA-C. (M6)**
- Task 3.1 Characterization of defects by D retention studies and MRE modelling - JSI, MPG, CEA, UHEL.
- Task 3.2 Development of C-NRA method - JSI, UHEL, MPG.
 - ❖ **O3.4 (Task 3.1 and Task 3.2) Detection of deuterium by C-NRA method. (M8)**
- Task 3.3 – Modelling of deuterium position in lattice/defect and identification of D position - UHEL, CEA, JSI.
 - ❖ **O3.5 (Task 3.3) Incorporation of C-NRA in RBSADEC. (M9)**

Positron annihilation lifetime spectroscopy



| Samples | Dose (dpa) | Temperature |
|---------|------------|-------------|
| 78d | 0.02 | 290 K |
| 78a | 0.2 | 290 K |
| 78h | 0.02 | 800 K |
| 78e | 0.2 | 800 K |
| 78i | 0 | Reference |

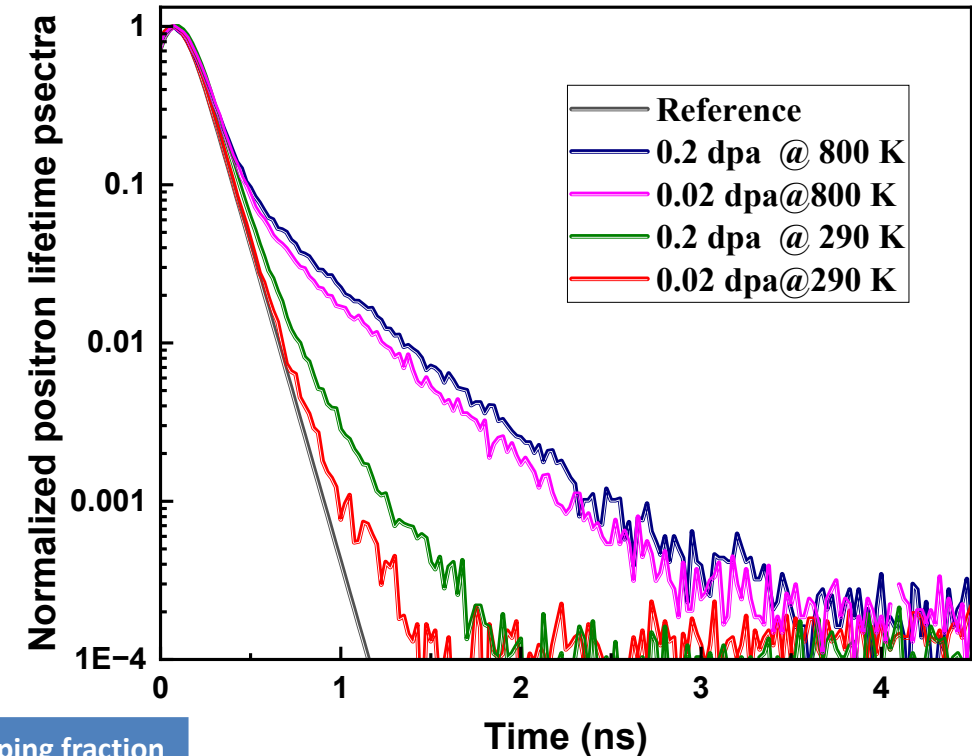


Lifetimes for irradiated samples

The average positron lifetime in the non-irradiated sample has been determined as 108 ps;

➤ **Excellent crystalline quality**

| Sample irradiation conditions | τ_{ave} (ps) | τ_1 (ps) | τ_2 (ps) | I_2 (%) | Trapping fraction (%) |
|-------------------------------|-------------------|---------------|---------------|------------|-----------------------|
| 2325K_ref. | 108.4 | 108 | -- | -- | -- |
| 0.02dpa_290K | 116.4 | 110 (2) | 224 (30) | 5.2 (2.5) | 7 |
| 0.2dpa_290K | 135.2 | 114 (1) | 265 (8) | 14.2 (1.3) | 17 |
| 0.02dpa_800K | 168.9 | 102 (1) | 429 (4) | 20.4 (0.4) | 19 |
| 0.2dpa_800K | 192.6 | 106 (1) | 453 (3) | 24.9 (0.3) | 24 |



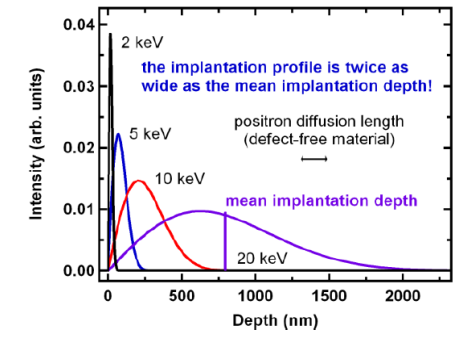
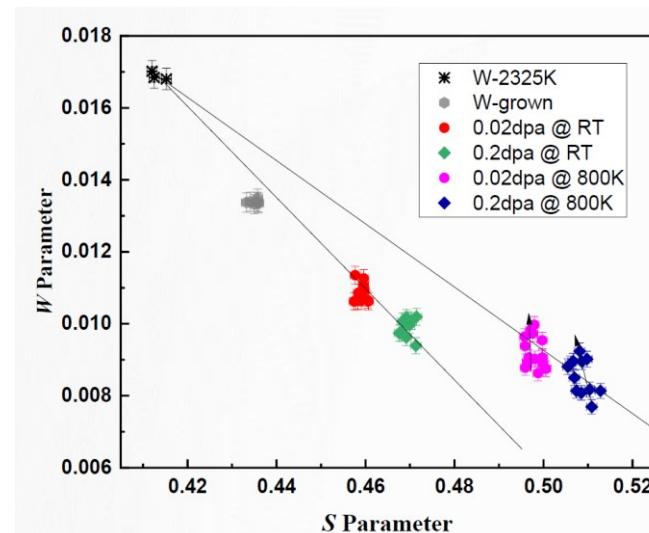
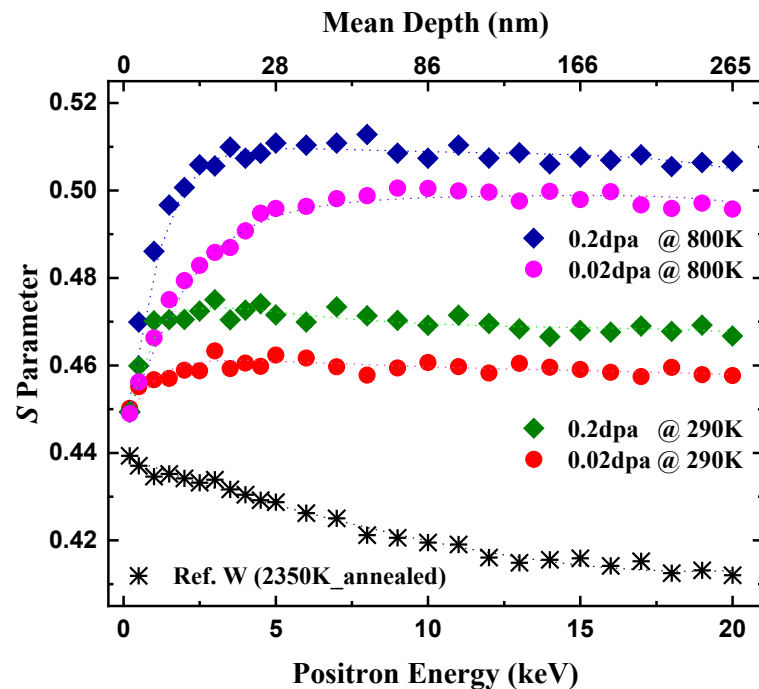
$V > 1$,
 $V_2 - V_4$
 $> V_{25}$

Single vacancy 160-200 ps
 [Yang 2022, Heikinheimo 2019]

Positron annihilation - Doppler broadening



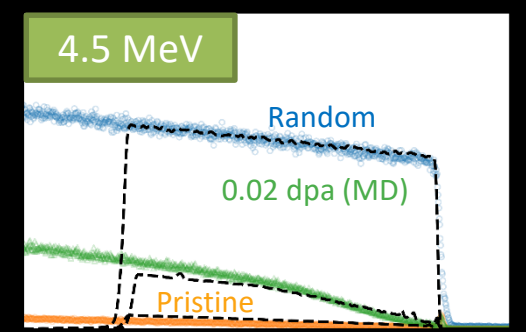
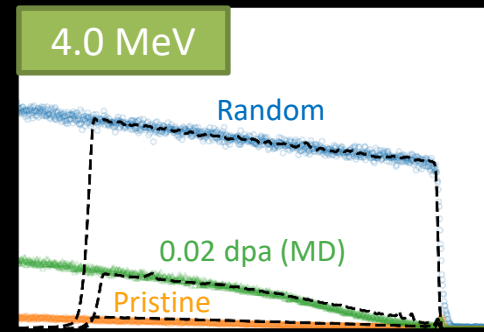
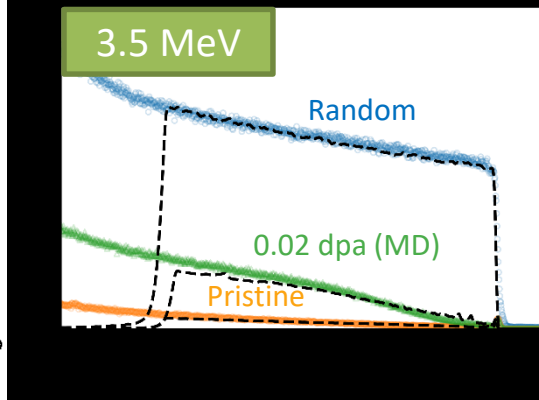
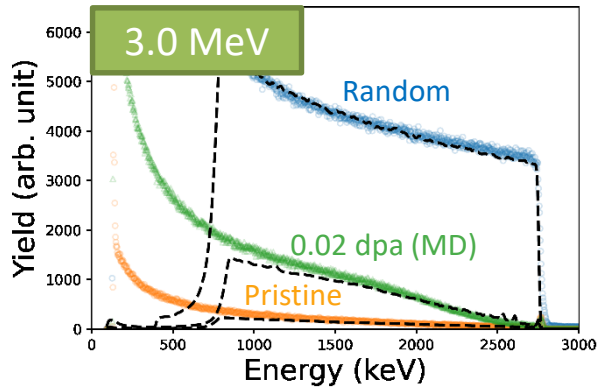
- The DBS measurements of positron annihilation radiation were performed on the same single crystal samples with a variable monoenergetic slow positron beam at the Institute of High Energy Physics, Chinese Academy of Science, China (IHEP).
- Positron implantation energies varied from 0.2 to 20 keV, corresponding to a mean penetration depth up to 0.27 μm (maximum information depth $\sim 0.5 \mu\text{m}$). The line-shape parameters, S and W, are integrated from the Doppler spectrum.



Tasks and objectives in 2023



- Task 1.1 Incorporation of the goniometer in the INSIBA experimental station – JSI.
- Task 1.2 Detection system for ion beam methods
 - ❖ **O3.1 (Task 1.1) C-RBS spectra obtained with new channeling set-up. (D1)**
- Task 2.1 Production of samples with dominant defects in the material – MPG and JSI.
- Task 2.2 Characterization of defects –UHEL, JSI, MPG.
- Task 2.3 Simulation and interpretation of C-RBS spectra - UHEL, CEA, JSI.
 - ❖ **O3.2 (Task 2.2, 2.3, 3.1) Defect identification by C-RBS and correlation to TEM and PAS measurements – report. (D2)**
- Task 2.4 In-situ C-RBS and sample heating – JSI
 - ❖ **O3.3 (Task 2.4) In-situ sample heating in INSIBA-C. (M6)**
- Task 3.1 Characterization of defects by D retention studies and MRE modelling - JSI, MPG, CEA, UHEL.
- Task 3.2 Development of C-NRA method - JSI, UHEL, MPG.
 - ❖ **O3.4 (Task 3.1 and Task 3.2) Detection of deuterium by C-NRA method. (M8)**
- Task 3.3 – Modelling of deuterium position in lattice/defect and identification of D position - UHEL, CEA, JSI.
 - ❖ **O3.5 (Task 3.3) Incorporation of C-NRA in RBSADEC. (M9)**



Step A. creation of radiation defects – Molecular dynamics simulation

Collision cascade

Primary knock-on atom: 10 keV

Size of MD cells: ~20nm

Overlapping of cascades: high damage dose (evolution of defects)

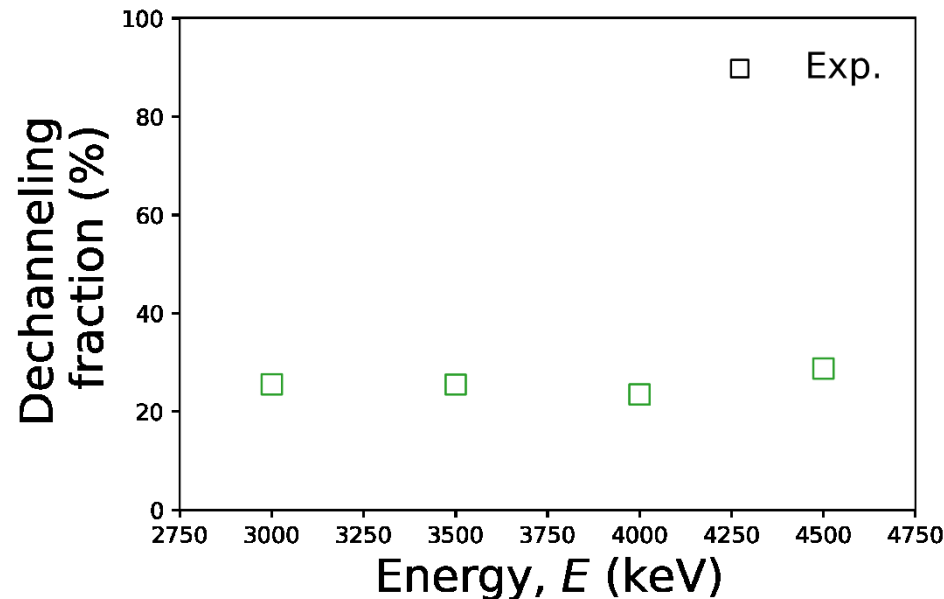
[F. Granberg et al., J. Nucl. Mater. 556 (2021) 153158]

Step B. Merge of MD cells – input for RBSADEC

Stack 70 MD cells along the [111] direction (the direction of depth)

The depth distribution of cascade number in the MD cells

Merge to one big cell (1.5 μm)

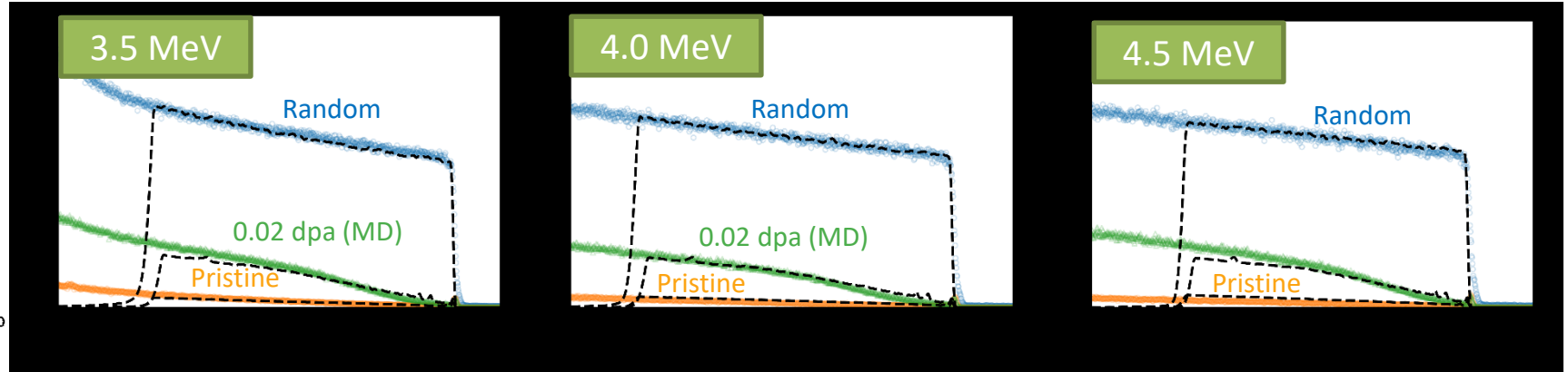
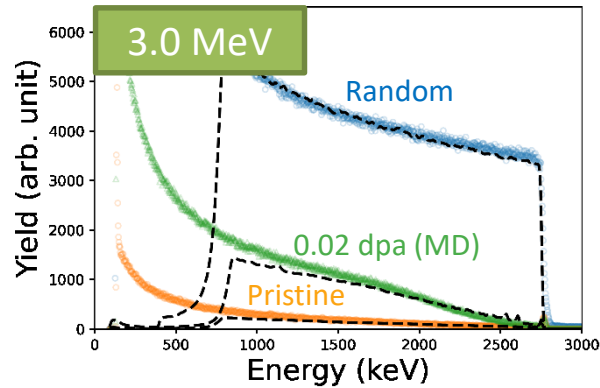


(Dechanneling calculated at 1.2 – 1.3 μm)

Dechanneling (energy)

Experiments: no obvious trend

Multi-energy RBS-C (0.02 dpa, 290 K)



Step A. creation of radiation defects – Molecular dynamics simulation

Collision cascade

Primary knock-on atom: 10 keV

Size of MD cells: ~20nm

Overlapping of cascades: high damage dose (evolution of defects)

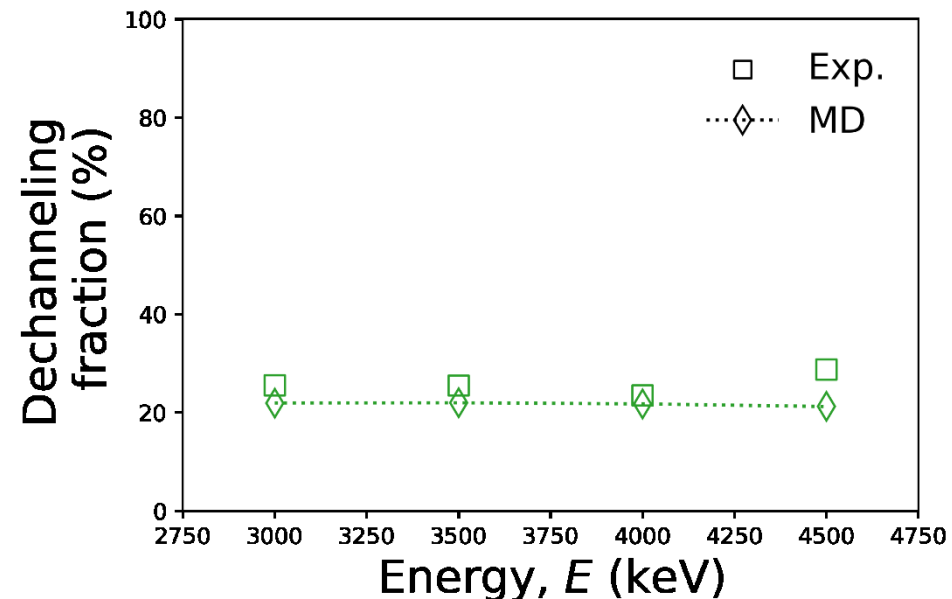
[F. Granberg et al., J. Nucl. Mater. 556 (2021) 153158]

Step B. Merge of MD cells – input for RBSADEC

Stack 70 MD cells along the [111] direction (the direction of depth)

The depth distribution of cascade number in the MD cells

Merge to one big cell (1.5 μm)

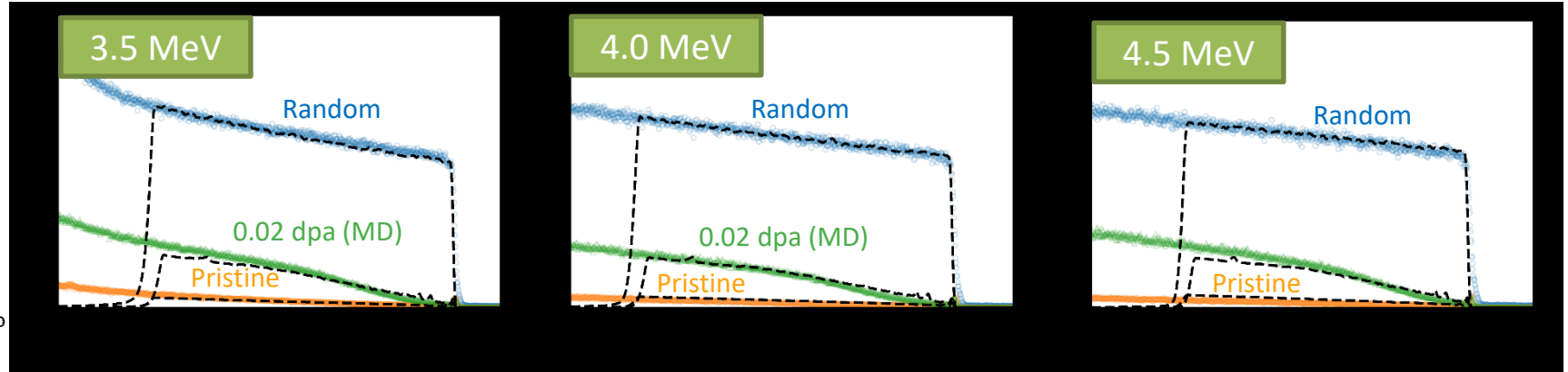
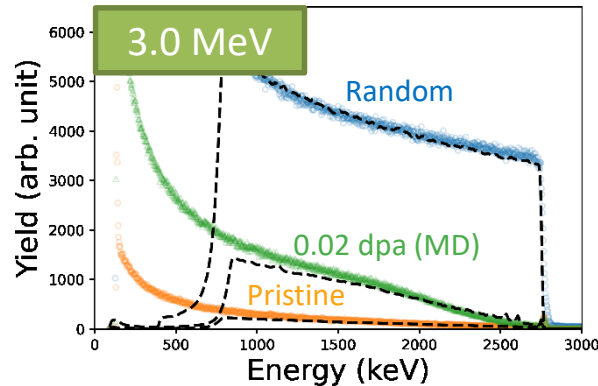


(Dechanneling calculated at 1.2 – 1.3 μm)

Dechanneling (energy)

- Experiments: no obvious trend
- Simulations (MD): constant

Multi-energy RBS-C (0.02 dpa, 290 K)



Step A. creation of radiation defects – Molecular dynamics simulation

Collision cascade

Primary knock-on atom: 10 keV

Size of MD cells: ~20nm

Overlapping of cascades: high damage dose (evolution of defects)

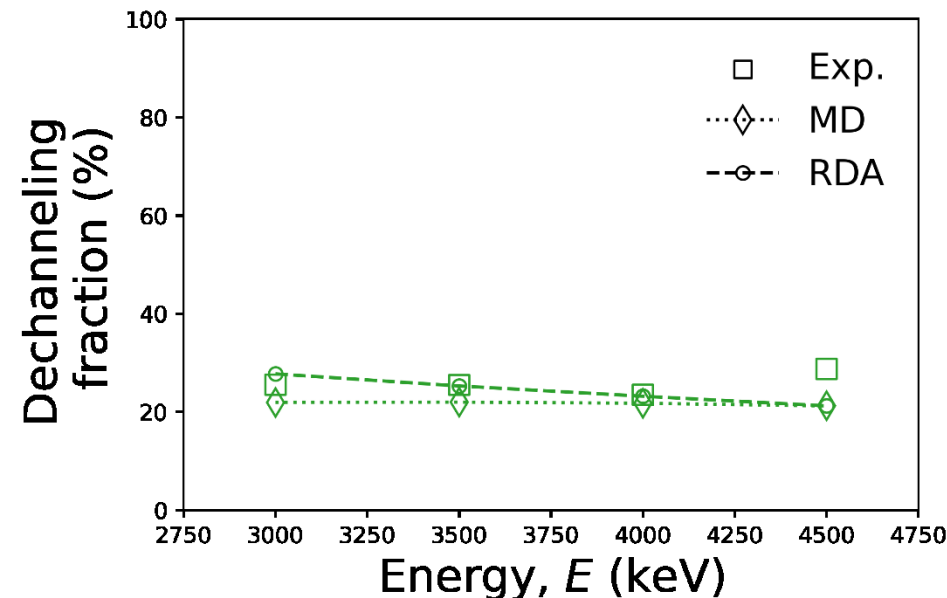
[F. Granberg et al., J. Nucl. Mater. 556 (2021) 153158]

Step B. Merge of MD cells – input for RBSADEC

Stack 70 MD cells along the [111] direction (the direction of depth)

The depth distribution of cascade number in the MD cells

Merge to one big cell (1.5 μm)



(Dechanneling calculated at 1.2 – 1.3 μm)

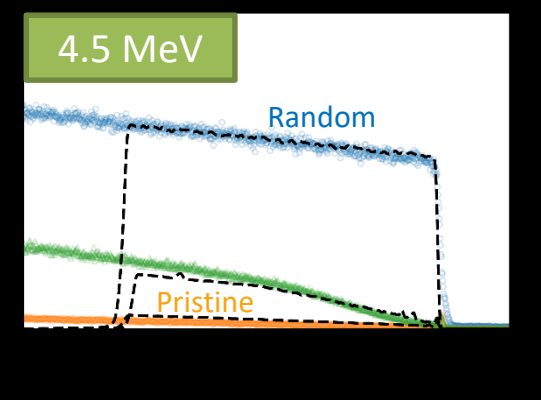
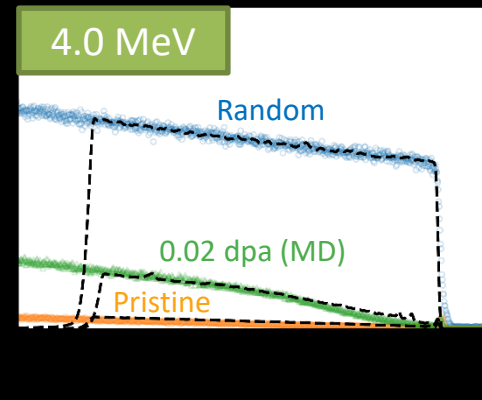
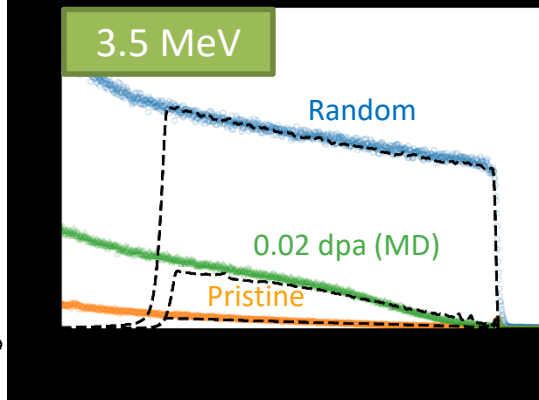
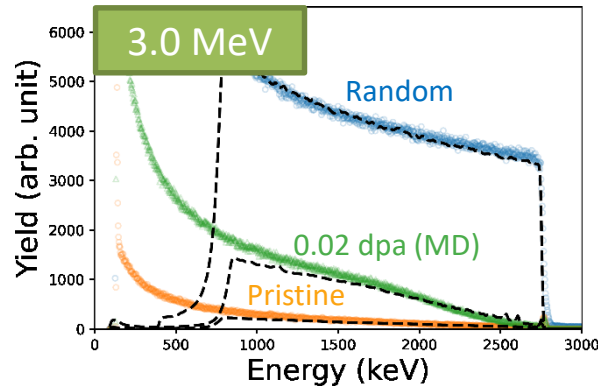
Dechanneling (energy)

- Experiments: no obvious trend
- Simulations (MD): constant
- Simulations (RDA): negative slope



Defect nature: dislocation loops

Multi-energy RBS-C (0.02 dpa, 290 K)



Step A. creation of radiation defects – Molecular dynamics simulation

Collision cascade

Primary knock-on atom: 10 keV

Size of MD cells: ~20nm

Overlapping of cascades: high damage dose (evolution of defects)

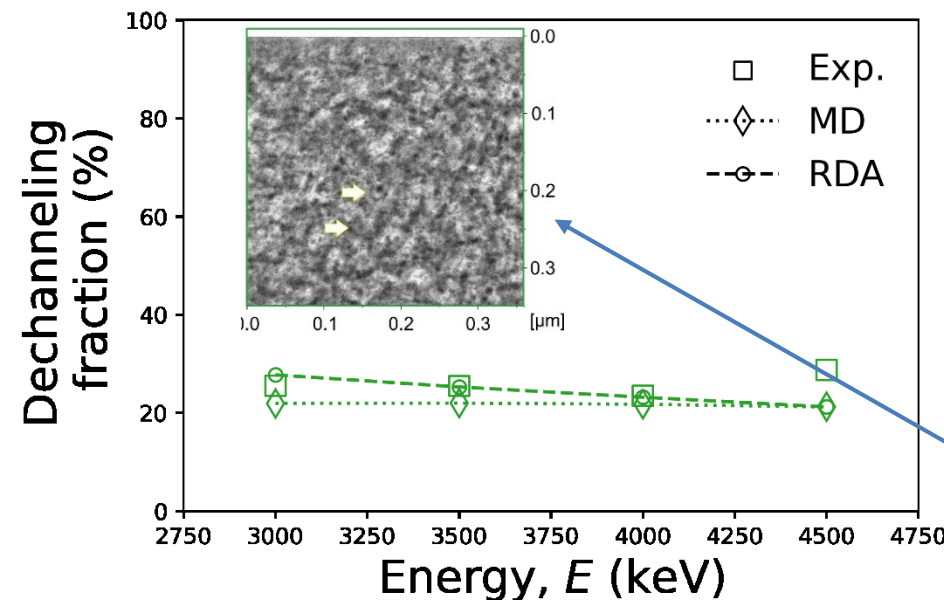
[F. Granberg et al., J. Nucl. Mater. 556 (2021) 153158]

Step B. Merge of MD cells – input for RBSADEC

Stack 70 MD cells along the [111] direction (the direction of depth)

The depth distribution of cascade number in the MD cells

Merge to one big cell (1.5 μm)



(Dechanneling calculated at 1.2 – 1.3 μm)

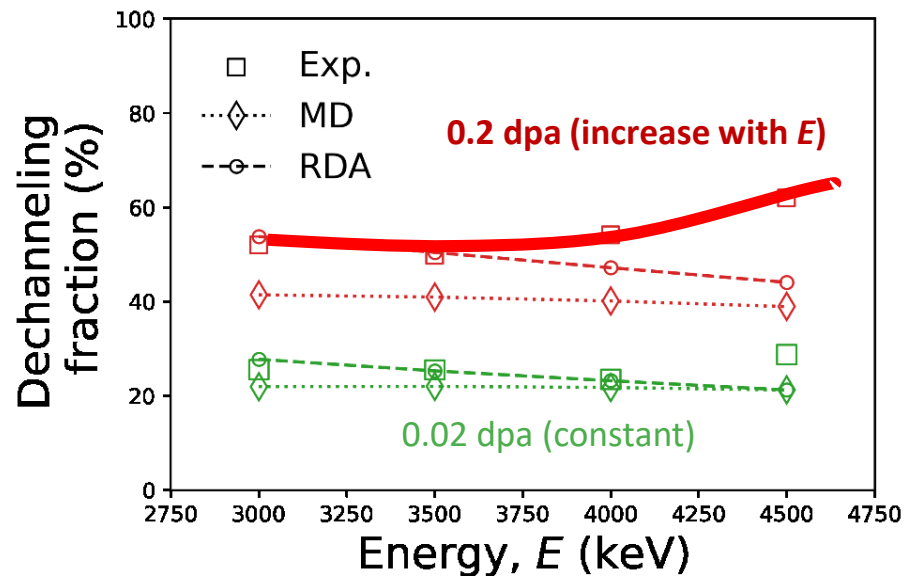
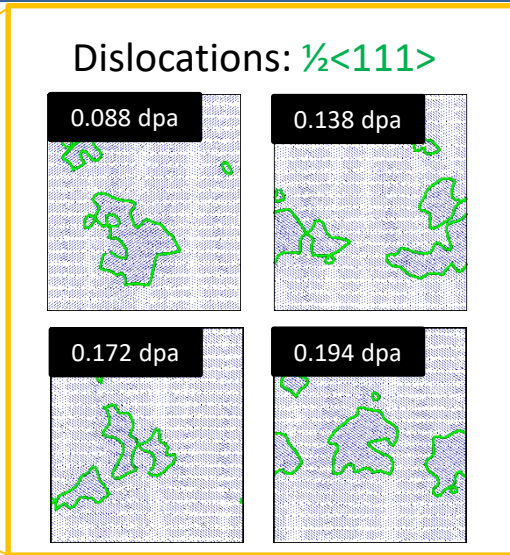
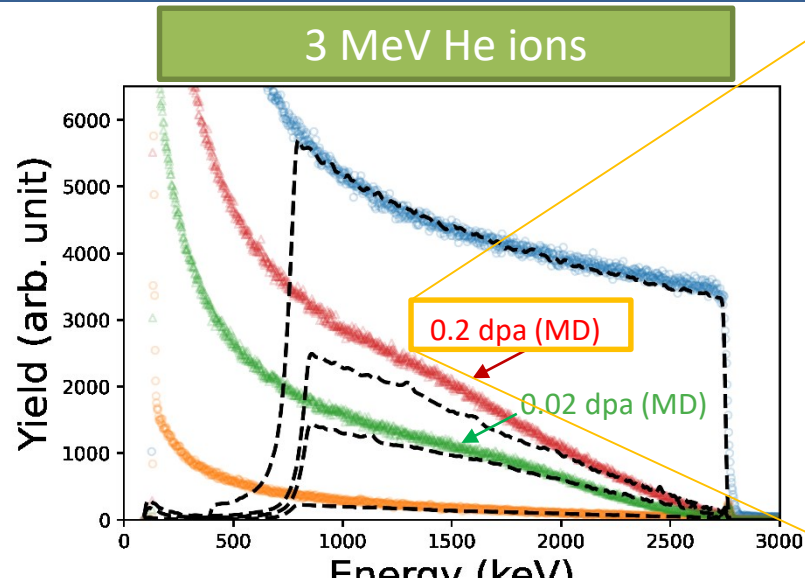
Dechanneling (energy)

- Experiments: no obvious trend
- Simulations (MD): constant
- Simulations (RDA): negative slope

Defect nature: dislocation loops

- STEM results:** U-shaped dislocation loops around “black dots” (size ~ 10 nm).

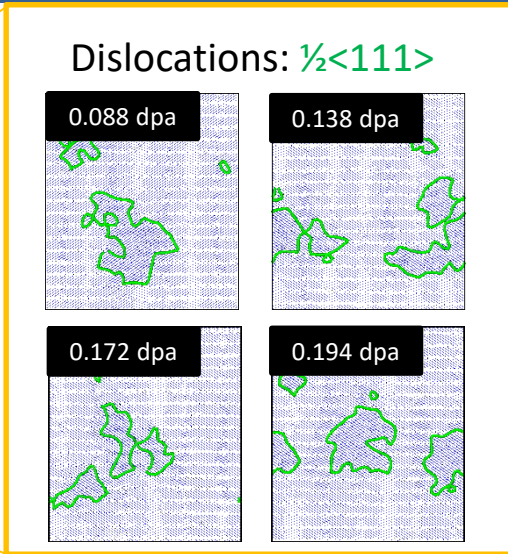
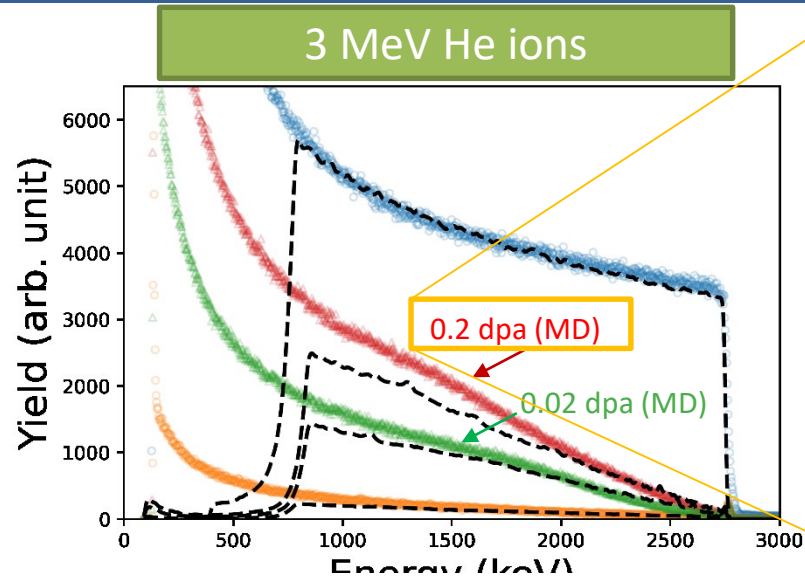
Multi-energy RBS-C (0.2 dpa, 290 K)



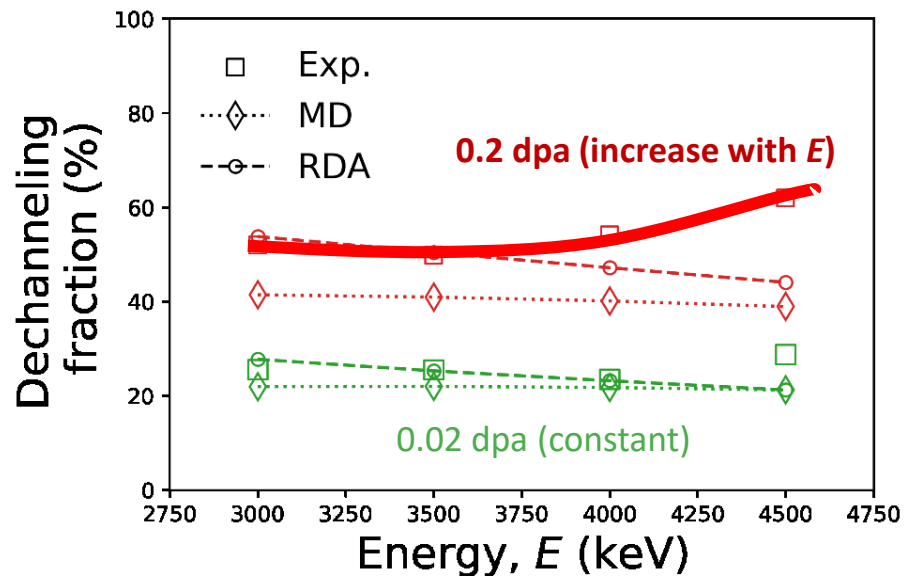
- RBS/c experiments (high damage, 0.2 dpa)
 - Higher yield than that of 0.02 dpa
- RBS/c simulations (MD cells)
- Dechanneling as a function of E

| | MD | Exp. | RDA |
|---------------|-------------------|--------------------|----------|
| Dechan. | Constant | Increases with E | Decrease |
| Defect nature | Dislocation loops | | |

Multi-energy RBS-C (0.2 dpa, 290 K)

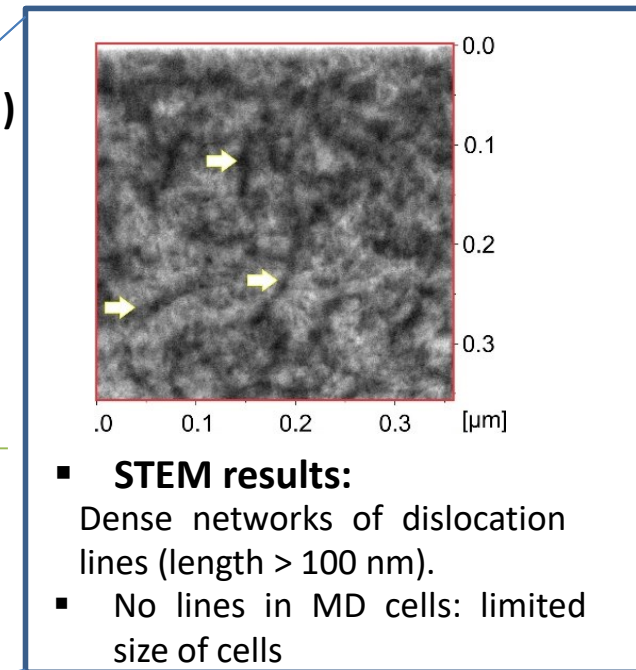


Lacking agreement between experiment and simulation due to limited size of MD cells – work in progress



- RBS/c experiments (high damage, 0.2 dpa)
 - Higher yield than that of 0.02 dpa
- RBS/c simulations (MD cells)
- Dechanneling as a function of E

| | MD | Exp. | RDA |
|---------------|-------------------|--------------------|----------|
| Dechan. | Constant | Increases with E | Decrease |
| Defect nature | Dislocation loops | Dislocation lines | |
| strain field | $1/r^3$ | $1/r$ | |





Acta Materialia 263 (2024) 119499



ELSEVIER

Contents lists available at ScienceDirect

Acta Materialia

journal homepage: www.elsevier.com/locate/actamat



Full length article

Unveiling the radiation-induced defect production and damage evolution in tungsten using multi-energy Rutherford backscattering spectroscopy in channeling configuration

S. Markelj^{a,*}, X. Jin^b, F. Djurabekova^b, J. Zavašnik^a, E. Punzón-Quijorna^a,
T. Schwarz-Selinger^c, M.L. Crespillo^d, G. García López^d, F. Granberg^b, E. Lu^b, K. Nordlund^b,
A. Šestan^a, M. Kelemen^a

^a Jožef Stefan Institute, Jamova cesta 39, 1000 Ljubljana, Slovenia

^b Department of Physics, University of Helsinki, Helsinki, Finland

^c Max-Planck-Institut für Plasmaphysik (IPP), Garching, Germany

^d Center for Micro Analysis of Materials (CMAM), Universidad Autónoma de Madrid (UAM), Cantoblanco, 28049-Madrid, Spain

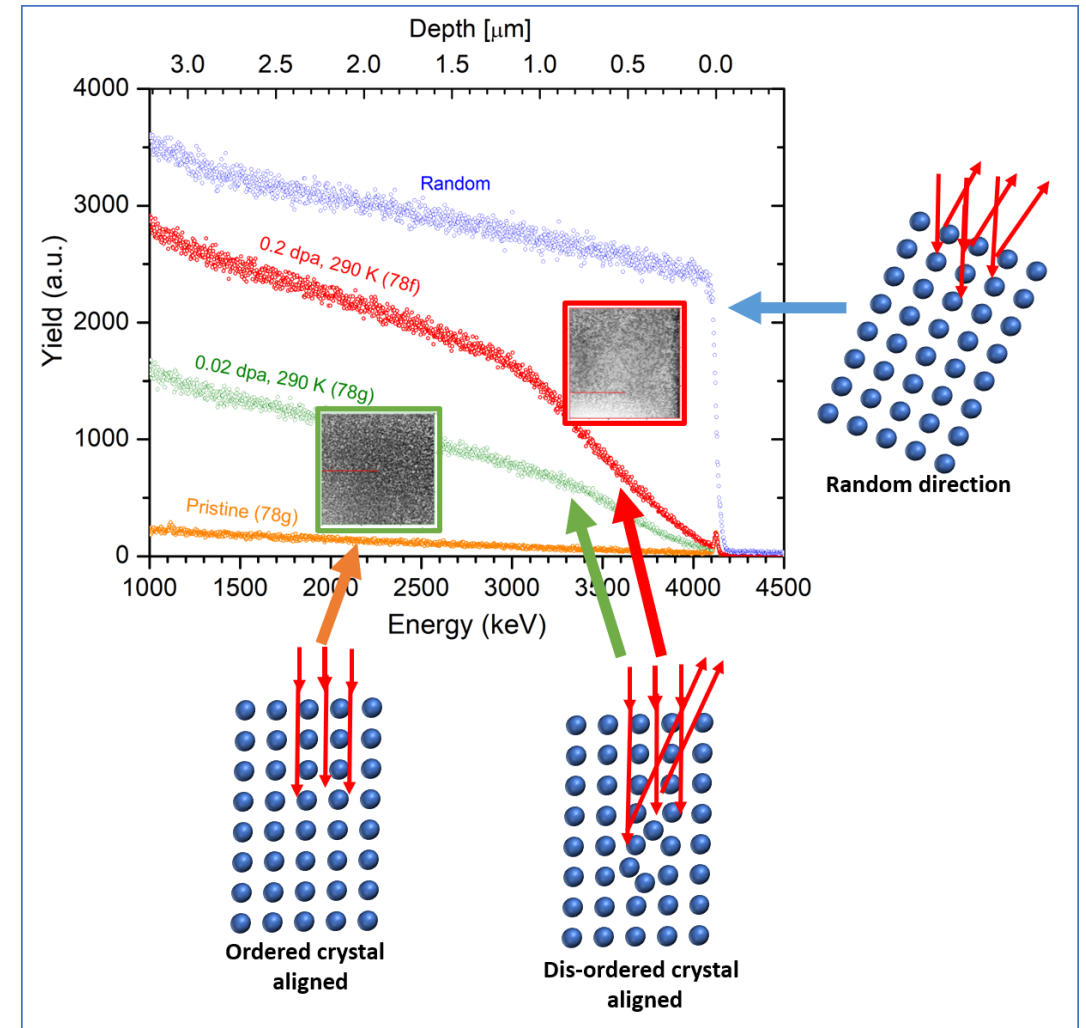
ARTICLE INFO

Keywords:

Tungsten
Defects
C-RBS
Displacement damage
Molecular dynamic simulations
TEM

ABSTRACT

Radiation-induced defect production in tungsten was studied by a combination of experimental and simulation methods. The analysis of structural defects was performed using multi-energy Rutherford backscattering spectroscopy in channeling configuration (multi-energy C-RBS). To create different microstructures, (111) tungsten (W) single crystals were irradiated with W ions at two different doses (0.02 and 0.2 dpa) at 290 K. Detailed transmission electron microscopy (TEM) analysis of the samples revealed the presence of dislocation lines and loops of different sizes. The RBSADEC code was used to simulate the measured C-RBS spectra, recorded with four different He beam energies along the (111) direction. For the first time for tungsten, molecular dynamics (MD) simulations of overlapping cascades were used as input. The well-known method of randomly displaced atoms (RDA) was applied for comparison. RDA does not provide a satisfactory understanding of the nature of the induced defect structure. With MD, a very good agreement between the simulated and experimental spectra was obtained for the sample prepared at a lower dose, despite the fact that the absolute defect densities are two orders of magnitude higher than those found with TEM. A discrepancy is observed for the high-dose-irradiated sample, which is ascribed to the presence of extended defects such as dislocation lines, which are clearly observed by TEM, but cannot be formed in finite size MD cells. RBSADEC with MD cells as input can describe correctly the response of the RBS signal with analysing beam energy while RDA as input gives the wrong trend.



Tasks and objectives in 2023

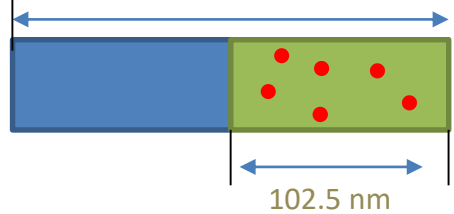


- Task 1.1 Incorporation of the goniometer in the INSIBA experimental station – JSI.
- Task 1.2 Detection system for ion beam methods
 - ❖ **O3.1 (Task 1.1) C-RBS spectra obtained with new channeling set-up. (D1)**
- Task 2.1 Production of samples with dominant defects in the material – MPG and JSI.
- Task 2.2 Characterization of defects –UHEL, JSI, MPG.
- Task 2.3 Simulation and interpretation of C-RBS spectra - UHEL, CEA, JSI.
 - ❖ **O3.2 (Task 2.2, 2.3, 3.1) Defect identification by C-RBS and correlation to TEM and PAS measurements – report. (D2)**
- Task 2.4 In-situ C-RBS and sample heating – JSI
 - ❖ **O3.3 (Task 2.4) In-situ sample heating in INSIBA-C. (M6)**
- Task 3.1 Characterization of defects by D retention studies and MRE modelling - JSI, MPG, CEA, UHEL.
- Task 3.2 Development of C-NRA method - JSI, UHEL, MPG.
 - ❖ **O3.4 (Task 3.1 and Task 3.2) Detection of deuterium by C-NRA method. (M8)**
- Task 3.3 – Modelling of deuterium position in lattice/defect and identification of D position - UHEL, CEA, JSI.
 - ❖ **O3.5 (Task 3.3) Incorporation of C-NRA in RBSADEC. (M9)**



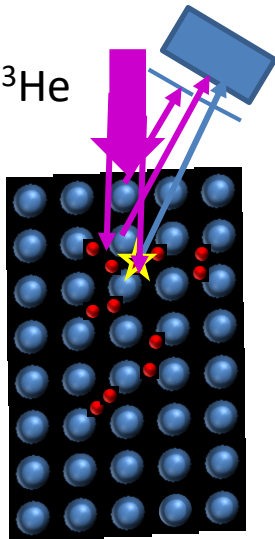
□ Incorporation of NRA-C into RBSADEC

- RBS-C: a pristine W target
- NRA-C:

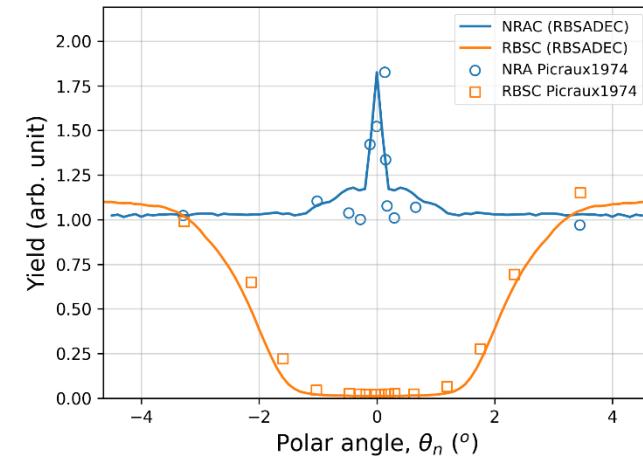
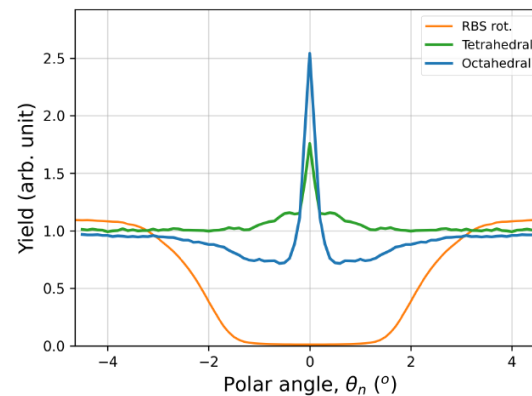
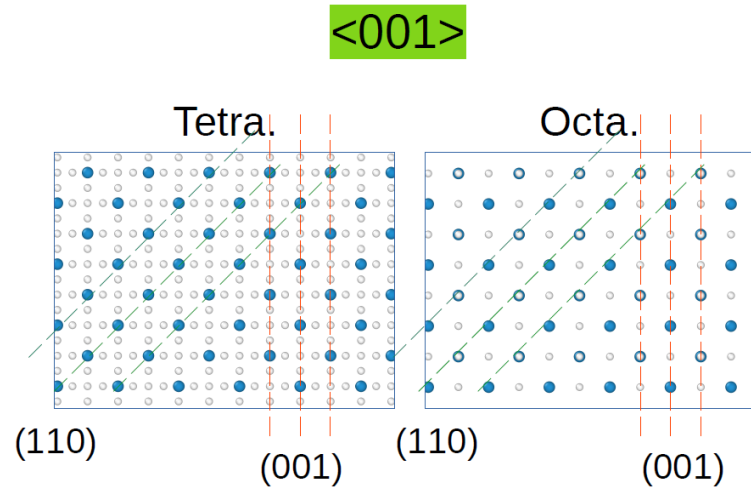


- 0.1 % of D at tetrahedral sites

750 keV ^3He



Angular scan



S. Picraux, Phys. Rev. Lett., 33, 1974)

$3 \times 10^{15} \text{ cm}^{-2}$ 30 keV D on W

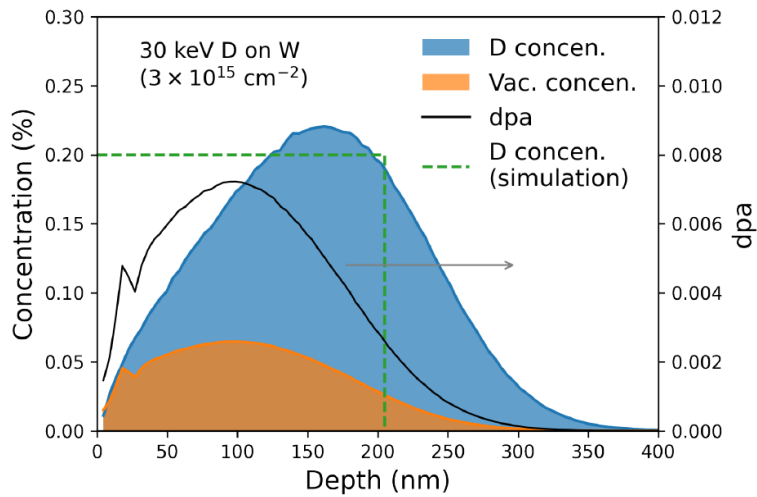
Difference between experiments and simulations: not exactly on tetrahedral sites? – Vacancies, some position close to tetrahedral sites, etc.

- Effect of damage dose: D sites change
- Improving the fit: adjust D locations, D location according to DFT calculations

Development of C-NRA simulation and detection of D by RBSADEC code

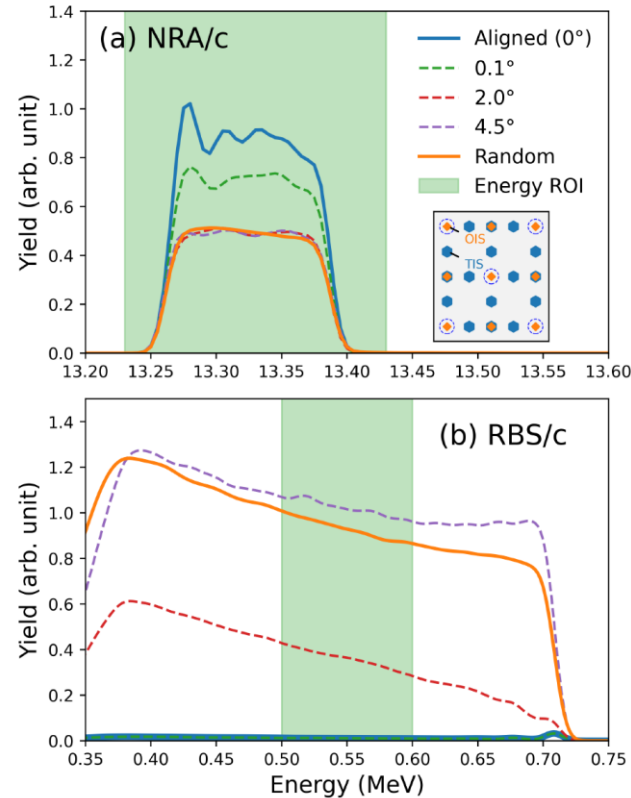
- SRIM calculation of vacancy distribution for 30 keV D ions in W for Picraux experiment

(S. Picraux, Phys. Rev. Lett., 33, 1974)

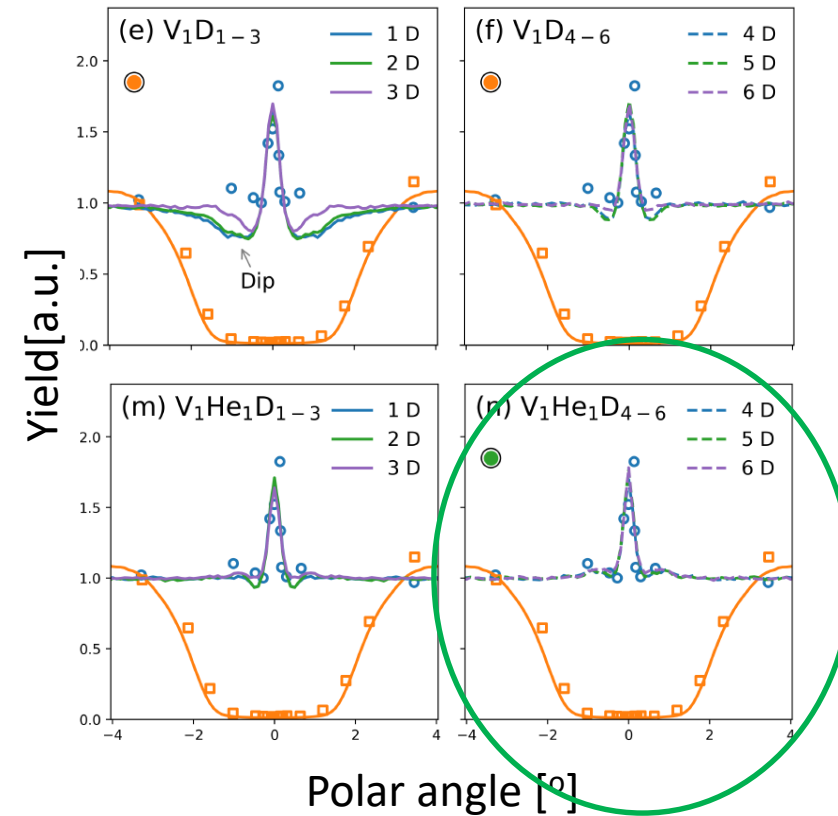


- Creation of vacancies
- Multiple hydrogen occupancy in a vacancy [Heinola et al. PR B (2010), Fernandez et al. Acta Materialia (2015)]
- Hydrogen occupancy for exp. conditions calculated by MHIMS

- Calculation the NRA and RBS yield



- Best agreement obtained for He-field vacancy with 5 H atoms



[Jin et al. submitted to PRM.]

Sample preparation - Tungsten single crystals



- Samples: NRA-C tungsten single crystals (100)

- Irradiation: 10.8 MeV W ions

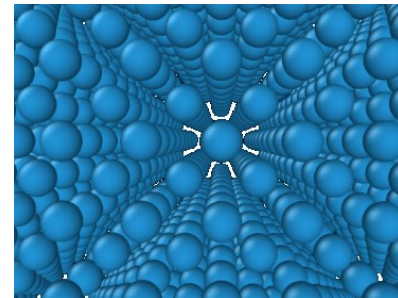
- **Two damage doses:**

Low ($5.8 \times 10^{16} m^{-2}$) & High ($5.8 \times 10^{17} m^{-2}$)

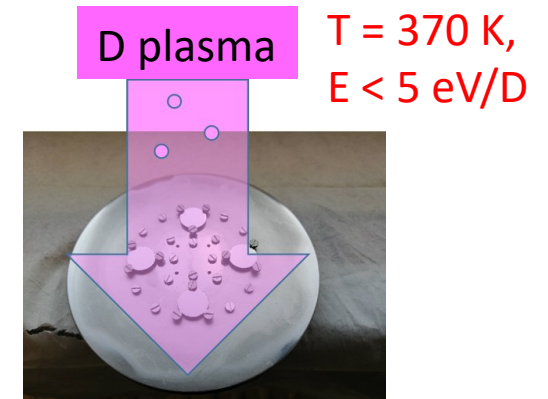
SRIM-KP

0.02 dpa

0.2 dpa



W (100)



Two temperatures:
290 K & 800 K

Single vacancies
@ low dose

Vacancy clusters
Diff. sizes

'gentle' loading = 'decoration' of defects
ion flux: $6 \times 10^{19} D/(m^2s)$
ion fluence: $1 \cdot 10^{25} D/m^2$ (48 h)

Based on Hu et al. JNM 556 (2022) 153175 – open volume type defects

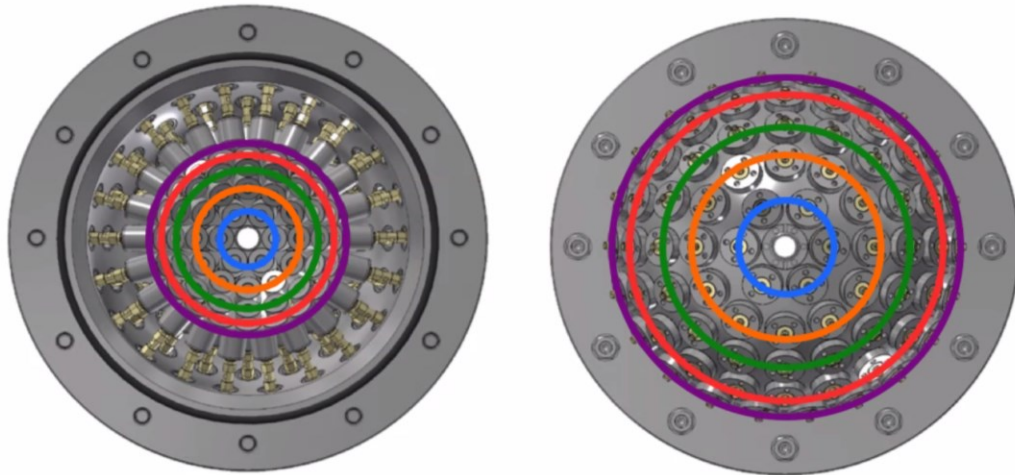
- W (100) single crystal should show a difference in the C-NRA signal when D is near the octahedral (OIS) or tetrahedral interstitial sites (TIS) [Cabstanjen, H.-D. Phys. Stat. Sol. (a) 59, 11–26 (1980)].

| Sample | Irradiation conditions | Predominant defect expected |
|----------|------------------------|-----------------------------|
| 78g / #1 | 0.02 dpa, 290 K | single vacancies |
| 78f / #5 | 0.2 dpa, 290K | heavily damaged standard |
| 78c / #3 | 0.02 dpa, 800 K | small vacancy clusters |
| 78b / #2 | 0.2 dpa, 800 K | big vacancy clusters |



Multi Detector RBS Setup

- Sensitive samples / insulating samples
- Higher **sensitivity** for trace elements
- Lateral **mapping**
- **Channeling** scans and **maps**
- Multiple backscattering angles to reduce the **ambiguity** of RBS

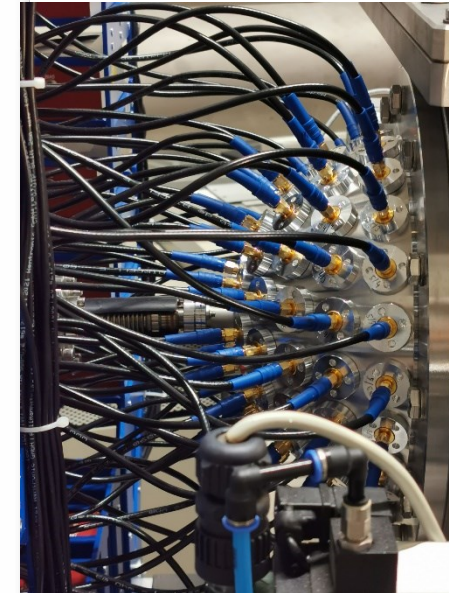


| | |
|-----|------------------|
| 6x | 165° = 53.8 msr |
| 12x | 150° = 107.6 msr |
| 16x | 135° = 143.5 msr |
| 20x | 120° = 179.3 msr |
| 22x | 105° = 197.3 msr |

$\Omega = 681.4 \text{ msr}$
9.2% of half sphere

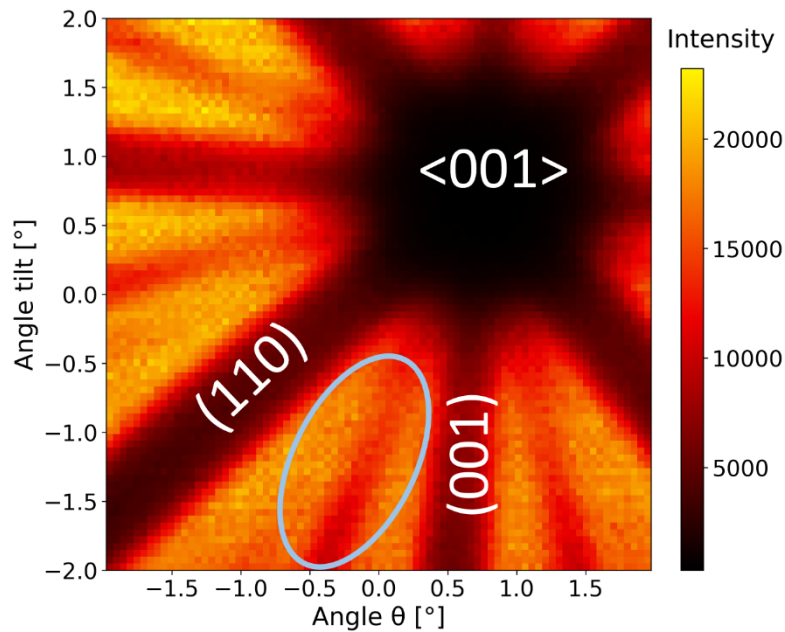


- 200 PIPS detectors fabricated @IBC

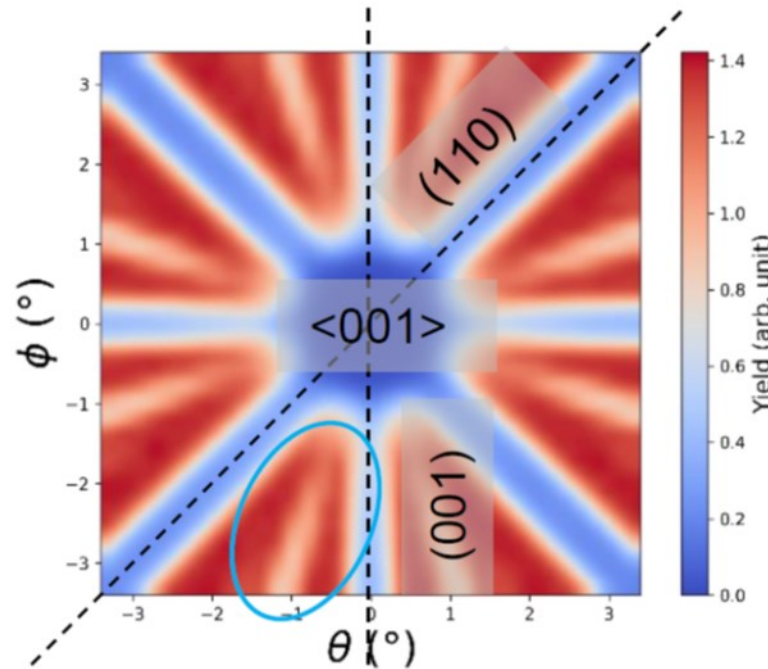


^4He 2.5 MeV RBS-C 2D maps / search for the channel

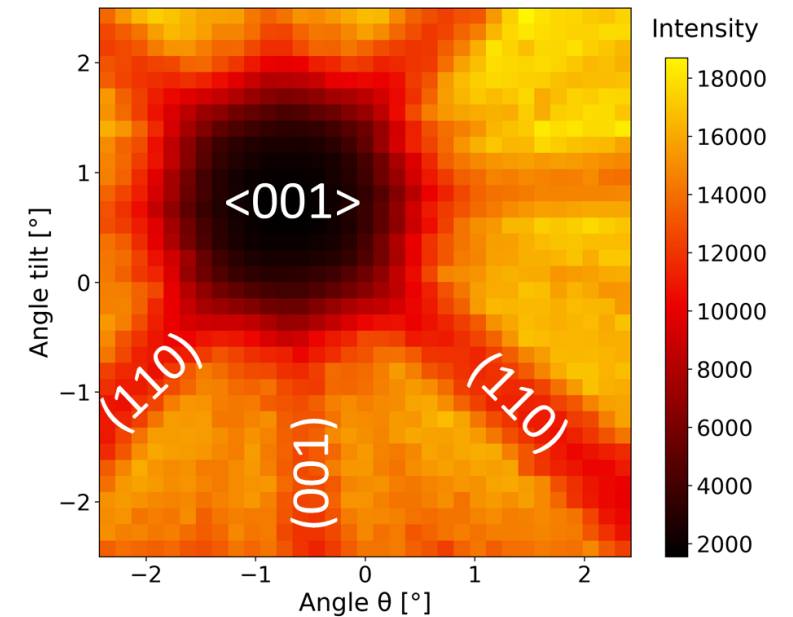
#4 - SC W (100) - Reference



Simulation – identification of channels



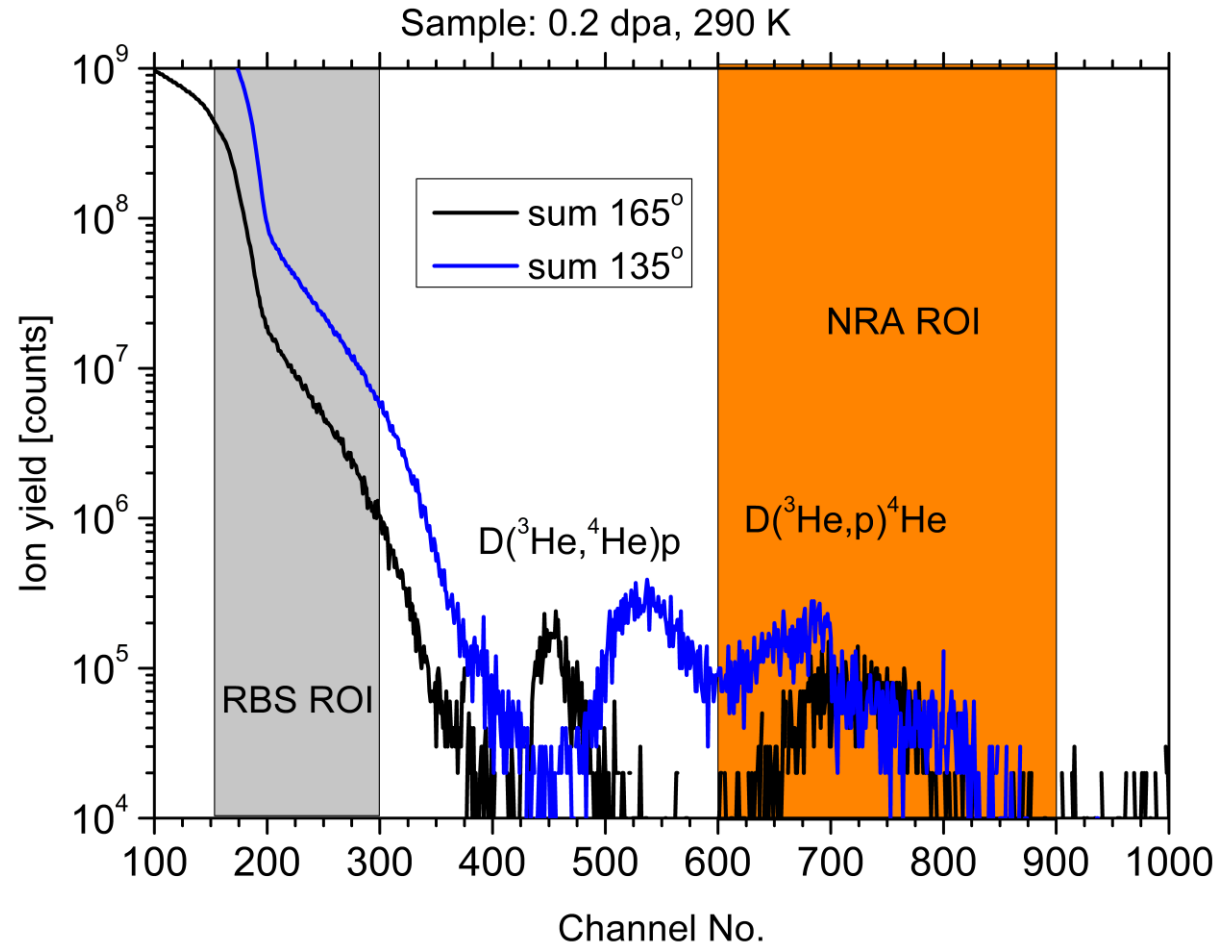
#5: 290 K, 0.2 dpa



Channels not well visible anymore for high irradiation dose

RBS-C was performed at the Hedgehog setup for RBS channeling at Ion beam center at HZDR.

^3He 0.8 MeV – simultaneous RBS-C and NRA-C 2D maps

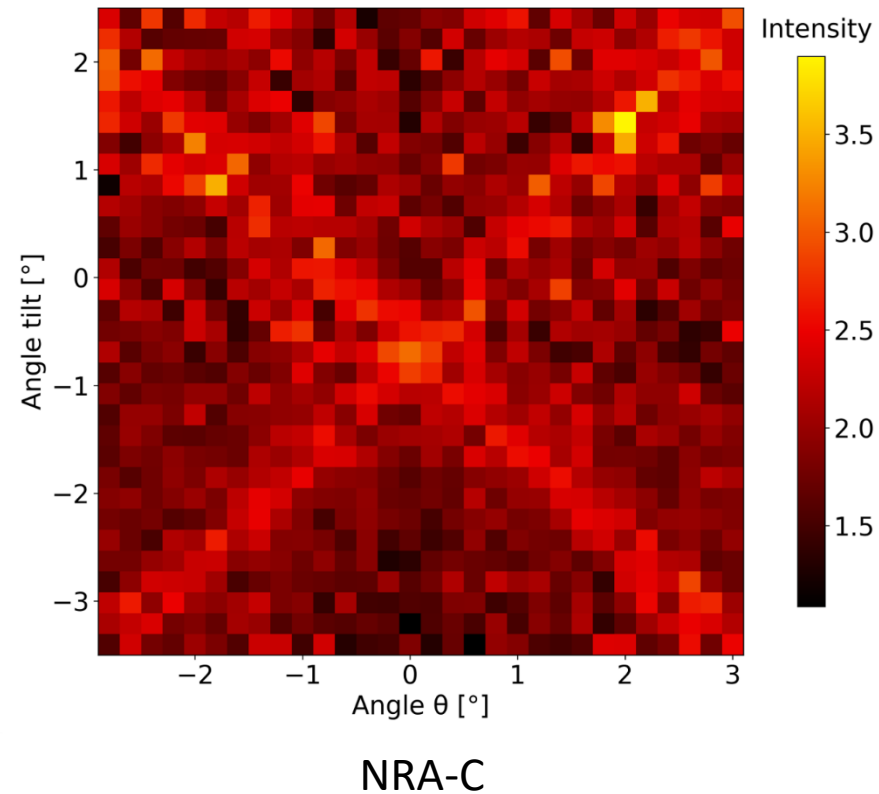
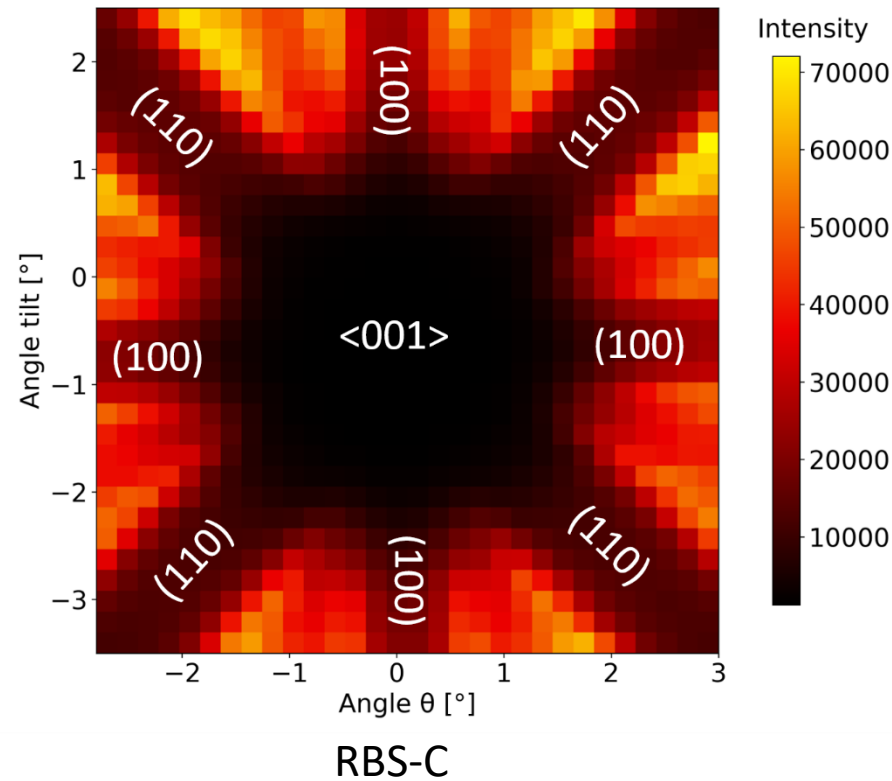


RBS-C was performed at the Hedgehog setup for RBS channeling at Ion Beam Center at HZDR.



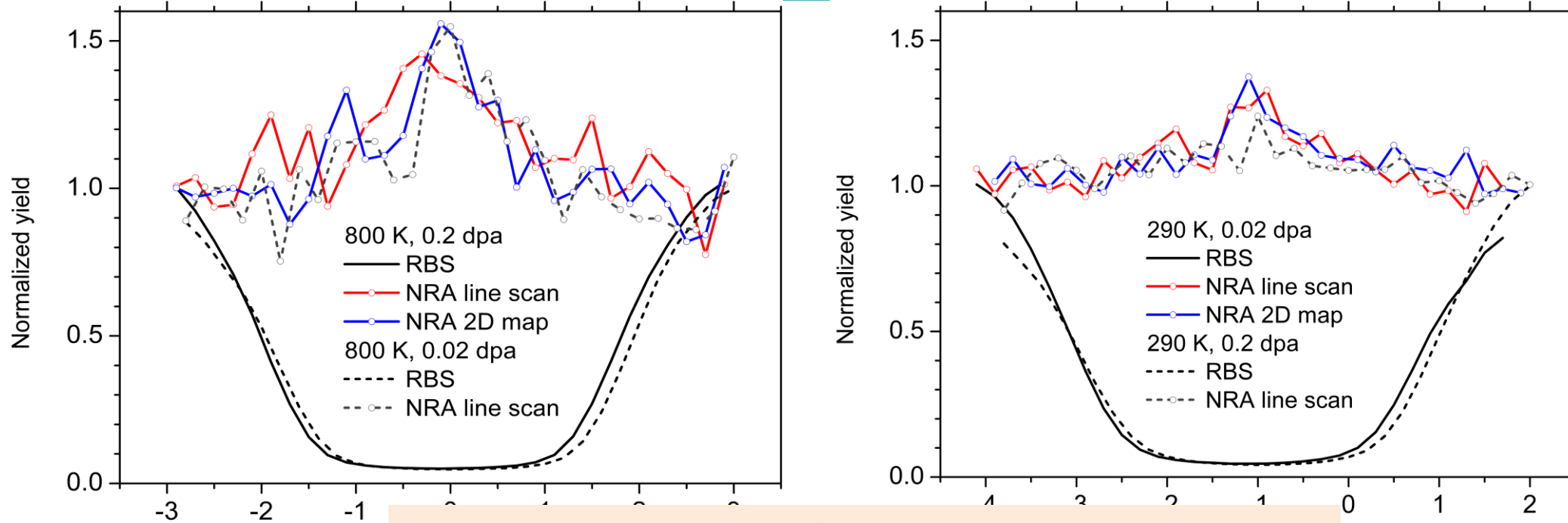
^3He 0.8 MeV – simultaneous RBS-C and NRA-C 2D maps

2D map for sample #2: 800 K, 0.2 dpa



RBS-C was performed at the Hedgehog setup for RBS channeling at Ion Beam Center at HZDR.

^3He 0.8 MeV – simultaneous RBS-C and NRA-C 2D maps



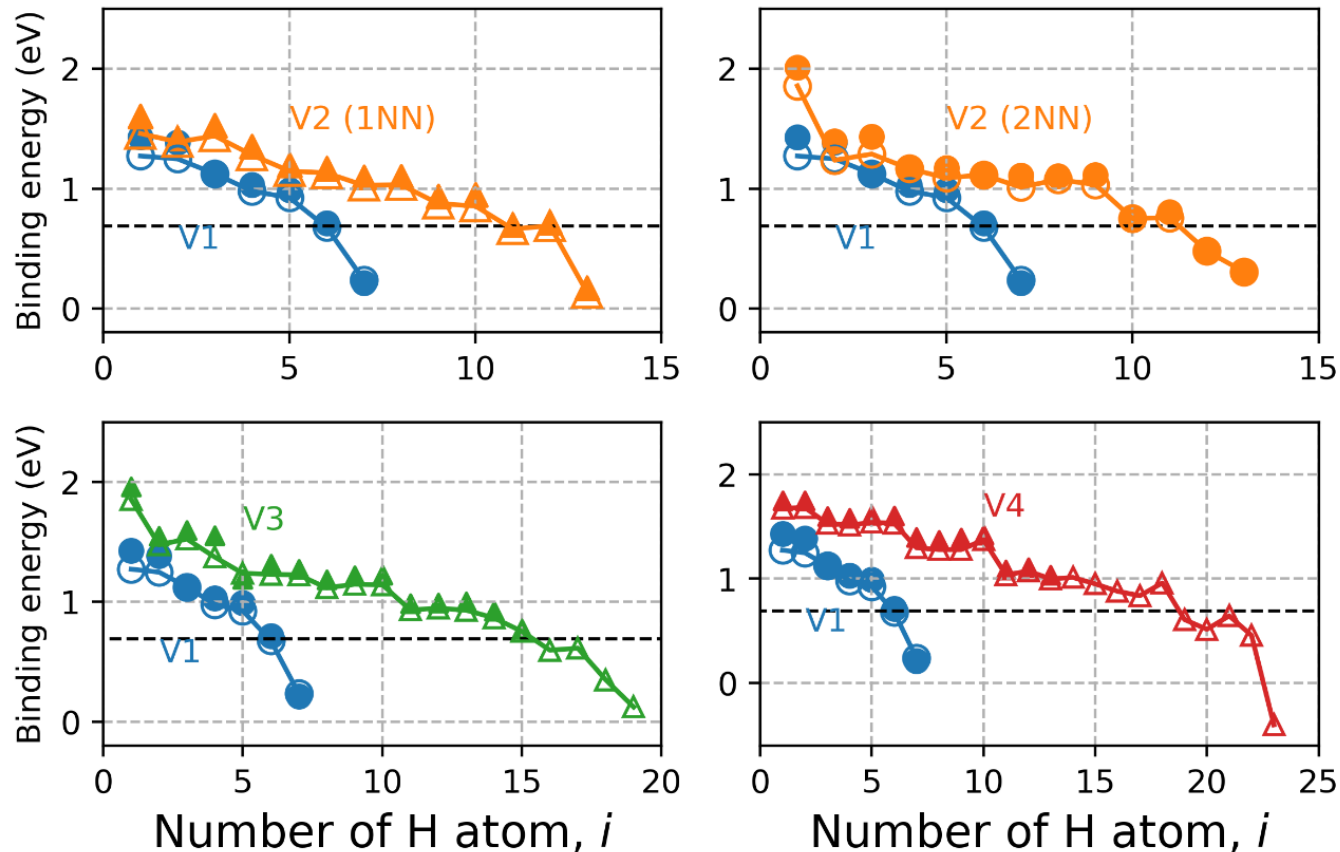
Work ongoing:

NRA-C simulations, combination with DFT - multi occupancy of H in vacancy and vacancy clusters

- The NRA signal peak is compared to the 0.02 dpa/290 K RBS signal compared
- Speculation: vacancy clusters are larger in size and the deuterium location in these clusters has a broader distribution, further away from the centre of the cluster.



■ Binding energy of H to $V_n H_{i-1}$



(empty and filled markers: energy without and with ZPE)

■ DFT calculations

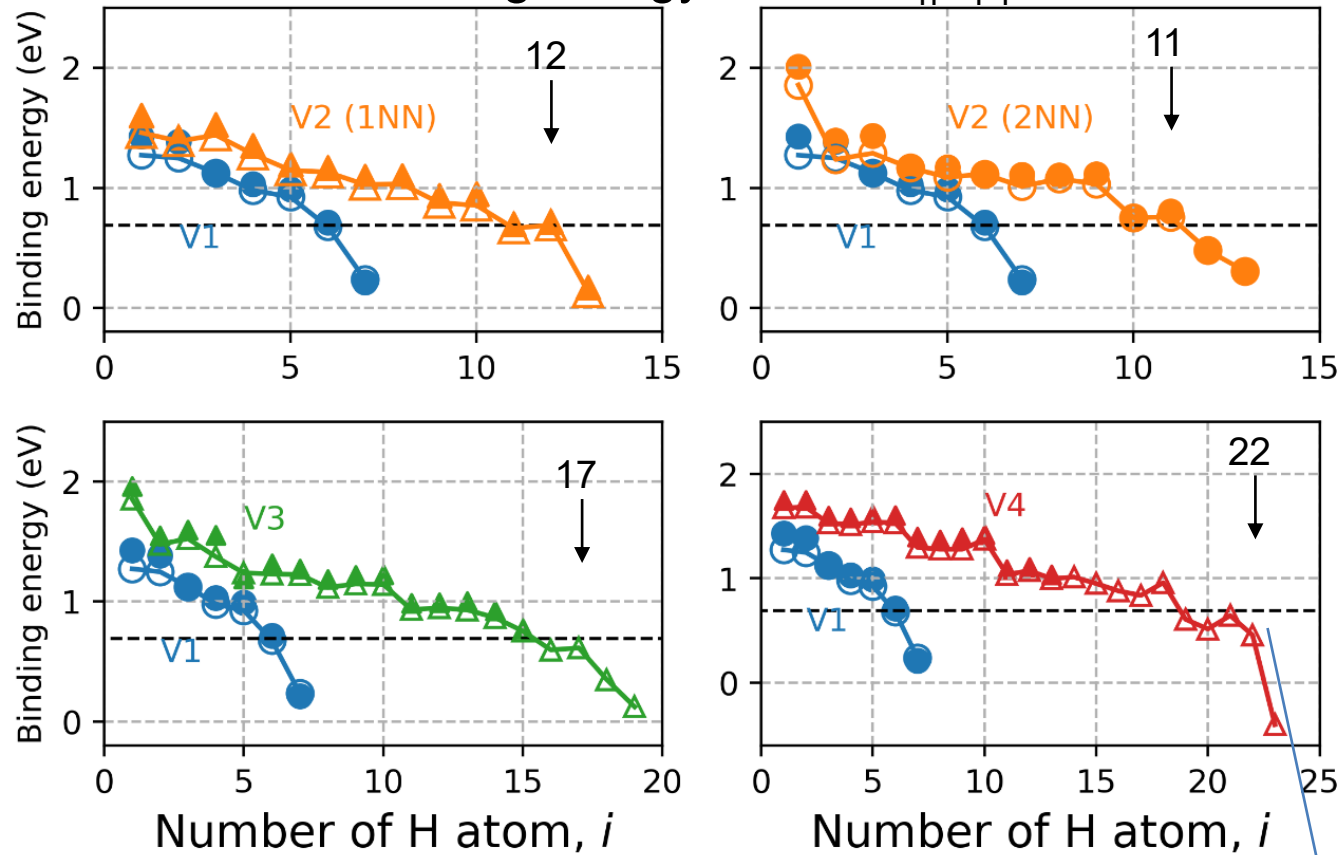
- VASP
- 4 * 4 * 4 supercell
- Cut-off energy: 500 eV
- Position and volume relaxation

- Estimation of the maximum number of H atoms attaching to the vacancy surface:
- Threshold binding energy of 0.69 eV (black dashed line)
(from N. Fernandez, et al., Acta Mater., 94, 2015)

DFT calculations of vacancy clusters



Binding energy of H to $V_n H_{i-1}$

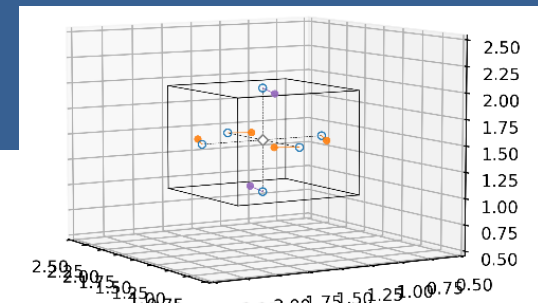


(empty and filled markers: energy without and with ZPE)

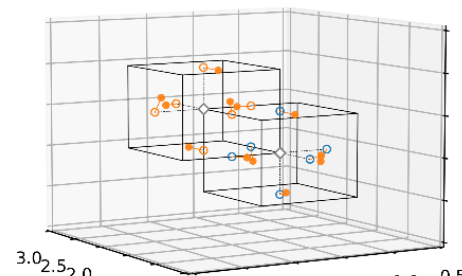
- Estimation of the maximum number of H atoms attaching to the vacancy surface: threshold binding energy of 0.69 eV (black dashed line)

(from N. Fernandez, et al., Acta Mater., 94, 2015)

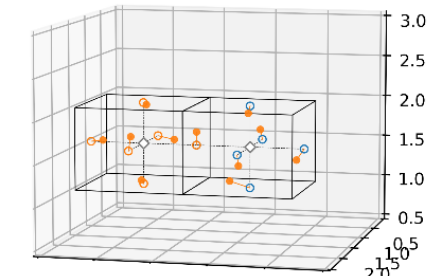
- Close relation to the number of vacancy faces



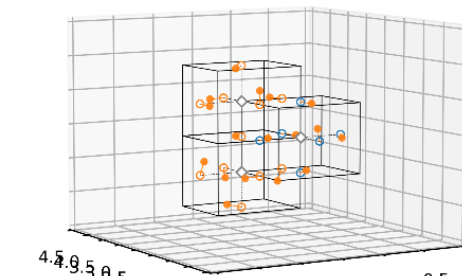
V1: 6 faces



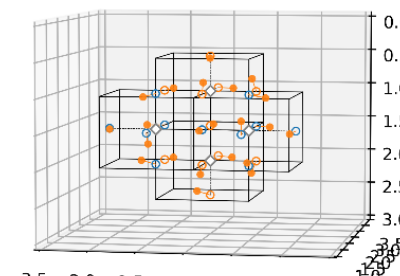
V2 (1NN): 12 faces



V2 (2NN): 11 faces



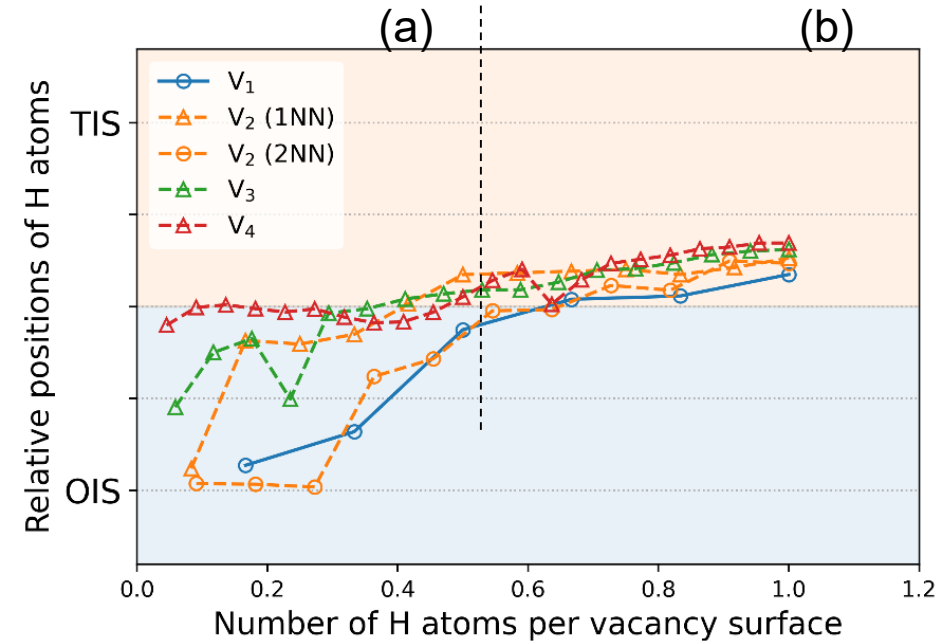
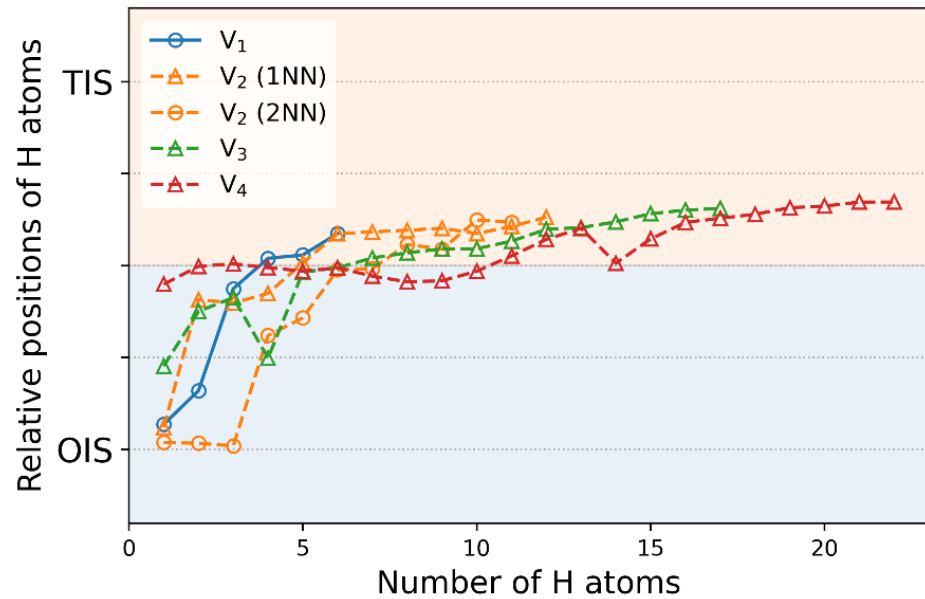
V3: 17 faces



V4: 22 faces



- Relative positions of H atoms between tetrahedral and octahedral sites



Change of H positions with the number of H atoms per vacancy surface:

(a): **< half filled**: clear different positions in different vacancy clusters

- Due to different types of vacancy surfaces

(b): **> half filled**: converge and get similar behavior.



PFMC conference:

- E. Punzon-Quijorna et al. "Multi-Energy Rutherford Backscattering Spectroscopy in Channeling configuration for the analysis of defects in tungsten" (poster)
- X. Jin et al. Study of the lattice location of deuterium implanted into tungsten using simulations of nuclear reaction analysis in channeling mode“(poster)

IBA conference:

- S Markelj et al., Analysis of deuterium and defects in tungsten by Rutherford backscattering spectroscopy and nuclear reaction analysis in channeling configuration“ (poster)
- X. Jin et al., Deuterium trapping conditions and potential location sites in tungsten by combination of nuclear reaction analysis in channeling mode with first principle calculations" (poster)
- F. Djurabekova et al., Simulation of Rutherford Backscattering spectrometry in channeling mode from arbitrary atomistic structures (Invited)

ICFRM conference:

- X. Jin et al., Analysis of radiation effects in tungsten by comparing molecular dynamics simulations to experiments of RBS-Channeling" (contributed talk)
- S Markelj et al., "Detection of defects and hydrogen by ion beam analysis in channeling mode for fusion - DeHydroC" (poster)

MINES:

- Markelj et al., Analysis of deuterium and defects in tungsten by Rutherford backscattering spectroscopy and nuclear reaction analysis in channeling configuration (Invited talk)



PSI conference May 2024:

- Markelj et al. Detection of defects and deuterium in displacement-damaged tungsten by applying Rutherford backscattering spectroscopy and nuclear reaction analysis in channeling configuration
- Hodille et al., Macroscopic modelling of D trapping in self-damaged tungsten with vacancy clusters using atomistic scale modelling data

Tasks and objectives in 2023



- Task 1.1 Incorporation of the goniometer in the INSIBA experimental station – JSI.
- Task 1.2 Detection system for ion beam methods
 - ❖ **O3.1 (Task 1.1)) C-RBS spectra obtained with new channeling set-up. (D1)**
- Task 2.1 Production of samples with dominant defects in the material – MPG and JSI.
- Task 2.2 Characterization of defects –UHEL, JSI, MPG.
- Task 2.3 Simulation and interpretation of C-RBS spectra - UHEL, CEA, JSI.
 - ❖ **O3.2 (Task 2.2, 2.3, 3.1) Defect identification by C-RBS and correlation to TEM and PAS measurements – report. (D2)**
- Task 2.4 In-situ C-RBS and sample heating – JSI
 - ❖ **O3.3 (Task 2.4) In-situ sample heating in INSIBA-C. (M6)**
- Task 3.1 Characterization of defects by D retention studies and MRE modelling - JSI, MPG, CEA, UHEL.
- Task 3.2 Development of C-NRA method - JSI, UHEL, MPG.
 - ❖ **O3.4 (Task 3.1 and Task 3.2) Detection of deuterium by C-NRA method. (M8)**
- Task 3.3 – Modelling of deuterium position in lattice/defect and identification of D position - UHEL, CEA, JSI.
 - ❖ **O3.5 (Task 3.3) Incorporation of C-NRA in RBSADEC. (M9)**



On schedule



Delayed



- Study of C-RBS during sample annealing.
- Paper on microstructure analysis and correlation with HI retention.
- Detection of deuterium in lattice defects and comparison to modelling.

Thank you for your attention

Multi energy C-RBS – experiment



- ^4He ions along $\langle 111 \rangle$ channel
- Multiple energies of He ions (3 MeV to 4.5 MeV) – **Multi energy RBS-C**

➤ RBS-C spectra @ 4.5 MeV

Irradiation at 290 K:

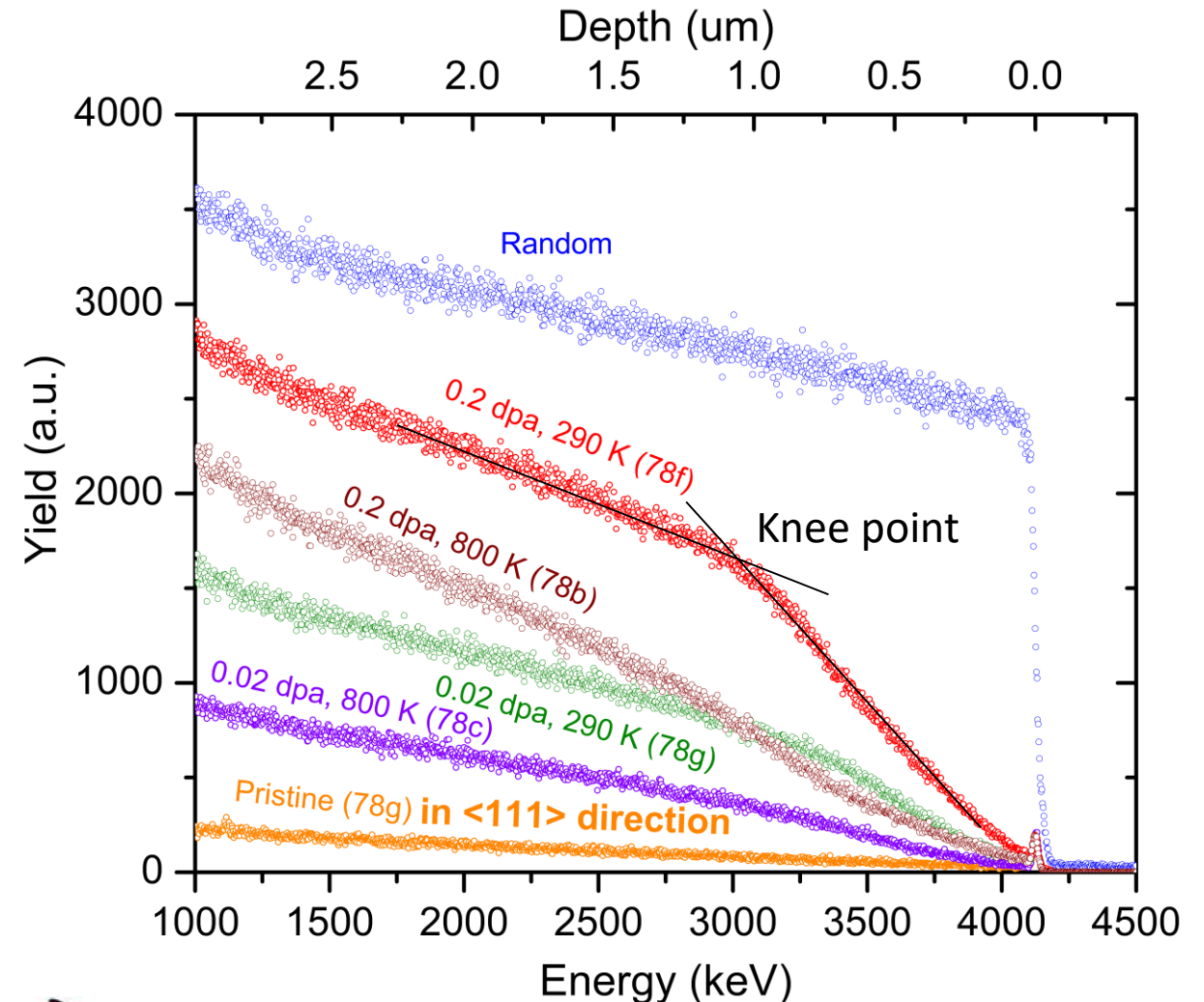
- 78f : 0.2 dpa, 290 K (heavily damaged standard)
- 78g : 0.02 dpa, 290 K (single vacancies)

Irradiation at 800 K:

- 78c : 0.02 dpa 800 K (small vacancy clusters)
- 78b : 0.2 dpa 800 K (big vacancy clusters)

- **Clear differences between the irradiation damage treatments**
- **Knee point indicates damage depth**

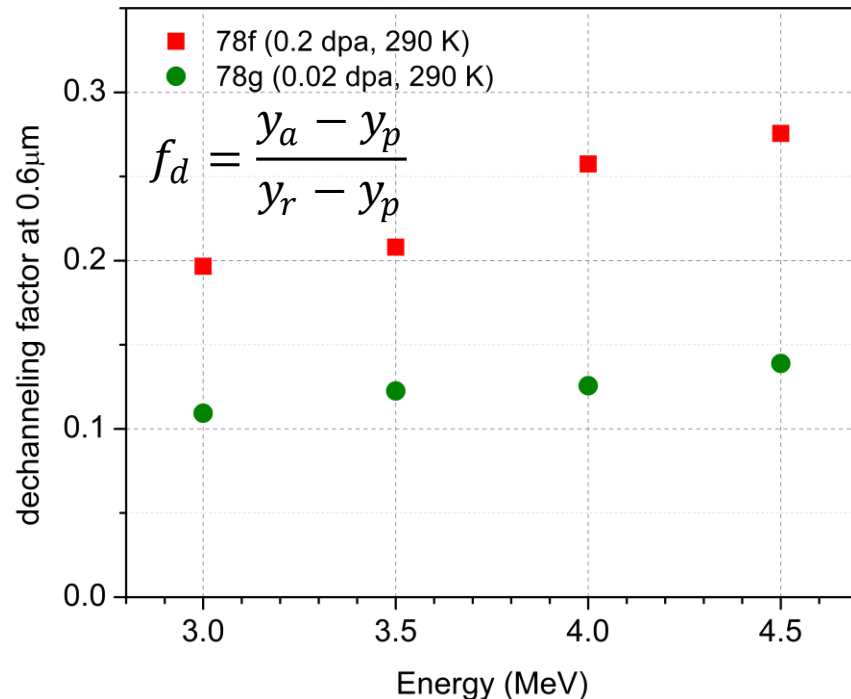
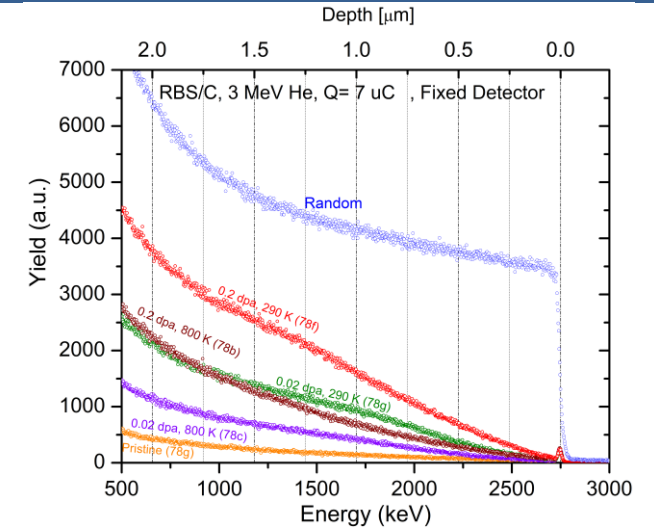
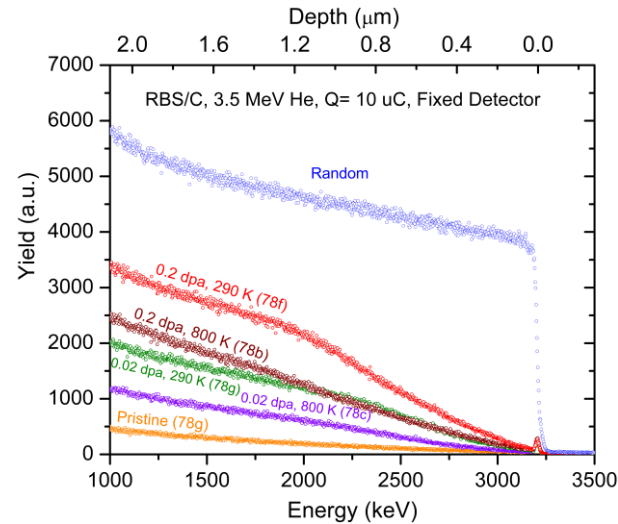
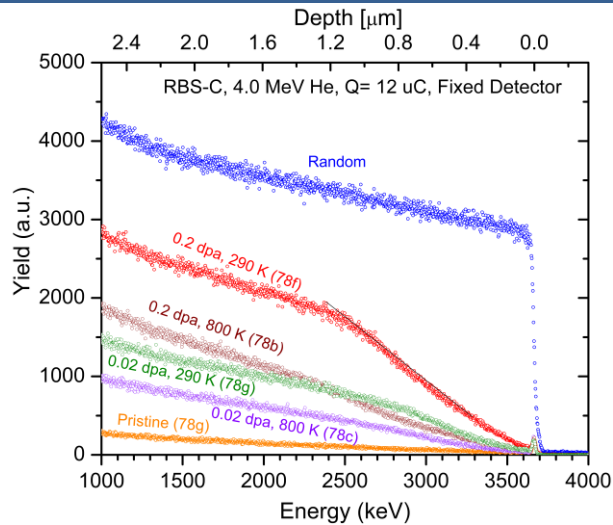
^4He beam $E=4.5$ MeV



Measurements were performed at CMAM, Madrid



Multi energy RBS-C



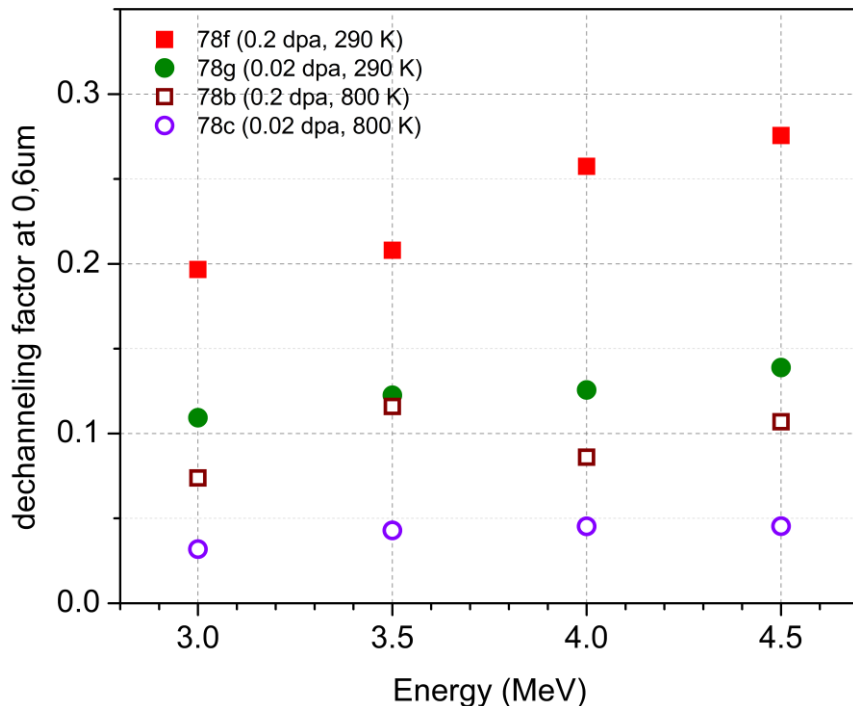
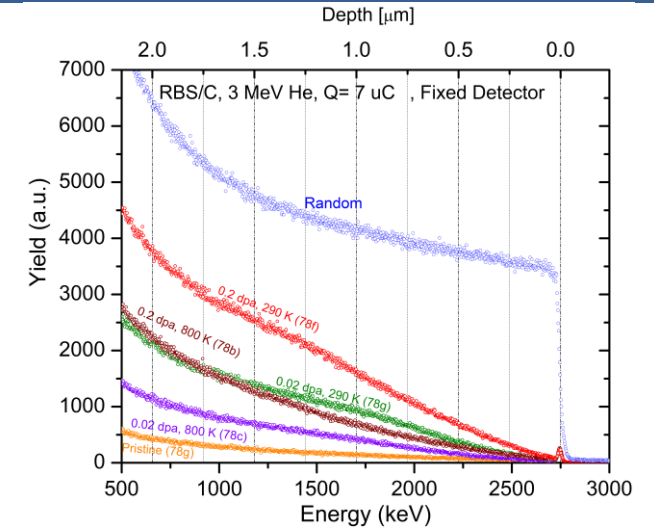
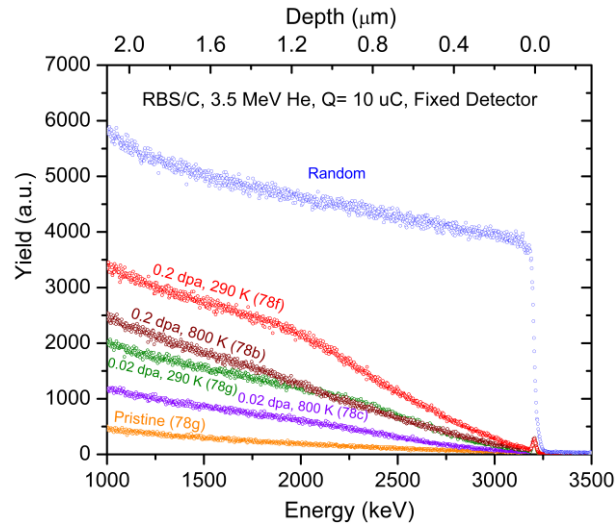
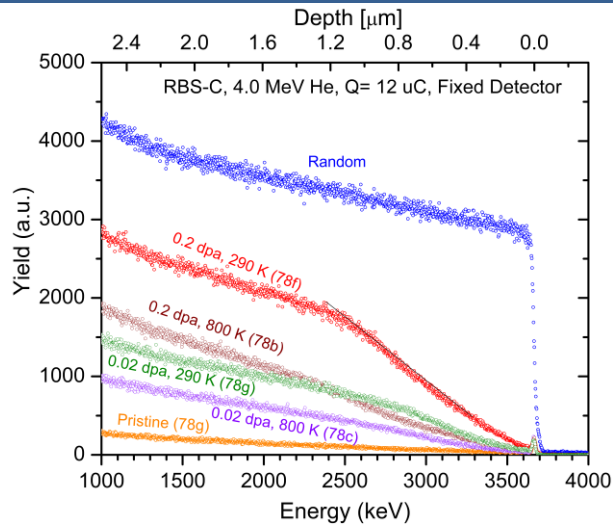
Dechanneling factor as a function of energy at 0.6 μm

78g (0.02 dpa, 290 K): no slope – discontinuous defects – small dislocation loops (TEM)

78f (0.2 dpa, 290 K): positive slope – extended defects – dislocation lines (TEM)

➤ Following: *FELDMAN, MATERIALS ANALYSIS BY ION CHANNELING. Submicron Crystallography, 1982, Academic press*

Multi energy RBS-C



Dechanneling factor as a function of energy at 0.6 μm

78g (0.02 dpa, 290 K): no slope – discontinuous defects – small dislocation loops (TEM)

78f (0.2 dpa, 290 K): positive slope – extended defects – dislocation lines (TEM)

78c (0.02 dpa, 800 K): no slope – discontinuous defects – dots and isolated lines (TEM)

78b (0.2 dpa, 800 K): no slope – discontinuous defects – (dislocation lines and black dots (TEM)

➤ Following: *FELDMAN, MATERIALS ANALYSIS BY ION CHANNELING. Submicron Crystallography, 1982, Academic press*